LEBANESE AMERICAN UNIVERSITY

Estimates of ground motion parameters of historical earthquakes in Lebanon based on the dynamic response of ancient free-standing columns using numerical and theoretical modeling.

By

Tamima Al Hassan

A thesis

Submitted in partial fulfillment of the requirements

for the degree of Master of Science in Engineering

School of Engineering

July 2022

LAU
الجامعة اللبنانية الأميركية
Lebanese American University

THESIS APPROVAL FORM

Student Name: Tamima AlHassan I.D. #: 202105035

Thesis Title: Estimates of ground motion parameters of historical earthquakes in Lebanon based on the dynamic response of ancient free-standing columns using numerical and theoretical modeling.

Program: Master of Science

Department: Civil Engineering

School: Engineering

The undersigned certify that they have examined the final electronic copy of this thesis and approved it in Partial Fulfillment of the requirements for the degree of:

Master of Science in the major of Civil and Environmental Engineering

Thesis Advisor's Name: Mazen Tabbara

Signature: [redacted] Date: 8 / 07 / 2022 (Day / Month / Year)

Committee Member's Name: Camille Issa

Signature: [redacted] Date: 8 / 07 / 2022 (Day / Month / Year)

Committee Member's Name: Caesar Abi Shdid

Signature: [redacted] Date: 8 / 07 / 2022 (Day / Month / Year)

LAU
الجامعة اللبنانية الأميركية
Lebanese American University

THESIS COPYRIGHT RELEASE FORM

LEBANESE AMERICAN UNIVERSITY NON-EXCLUSIVE DISTRIBUTION LICENSE

By signing and submitting this license, you (the author(s) or copyright owner) grants the Lebanese American University (LAU) the non-exclusive right to reproduce, translate (as defined below), and/or distribute your submission (including the abstract) worldwide in print and electronic formats and in any medium, including but not limited to audio or video. You agree that LAU may, without changing the content, translate the submission to any medium or format for the purpose of preservation. You also agree that LAU may keep more than one copy of this submission for purposes of security, backup and preservation. You represent that the submission is your original work, and that you have the right to grant the rights contained in this license. You also represent that your submission does not, to the best of your knowledge, infringe upon anyone's copyright. If the submission contains material for which you do not hold copyright, you represent that you have obtained the unrestricted permission of the copyright owner to grant LAU the rights required by this license, and that such third-party owned material is clearly identified and acknowledged within the text or content of the submission. IF THE SUBMISSION IS BASED UPON WORK THAT HAS BEEN SPONSORED OR SUPPORTED BY AN AGENCY OR ORGANIZATION OTHER THAN LAU, YOU REPRESENT THAT YOU HAVE FULFILLED ANY RIGHT OF REVIEW OR OTHER OBLIGATIONS REQUIRED BY SUCH CONTRACT OR AGREEMENT. LAU will clearly identify your name(s) as the author(s) or owner(s) of the submission, and will not make any alteration, other than as allowed by this license, to your submission.

Name: Tamima Al Hassan

Signature: [redacted] Date: 8 / 09 / 2022
Day Month Year

LAU
الجامعة اللبنانية الأميركية
Lebanese American University

PLAGIARISM POLICY COMPLIANCE STATEMENT

I certify that:

1. I have read and understood LAU's Plagiarism Policy.
2. I understand that failure to comply with this Policy can lead to academic and disciplinary actions against me.
3. This work is substantially my own, and to the extent that any part of this work is not my own I have indicated that by acknowledging its sources.

Name: Tamima Al Hassan

Signature: [redacted]

Date: 8 / 09 / 2022
Day Month Year

ACKNOWLEDGMENT

I would like to thank my thesis advisor, Dr. Mazen Tabbara, for his effort, continuous support, and guidance during the research process.

I would also like to thank the committee members, Dr. Caesar Abi Shdid and Dr. Camille Issa, for their counseling and support.

Estimates of ground motion parameters of historical earthquakes in Lebanon based on the dynamic response of ancient free-standing columns using numerical and theoretical modeling.

Tamima Al Hassan

ABSTRACT

Lebanon has been devastated by large earthquakes over the last ten centuries, the last two major earthquakes hit Lebanon in 1202 and 1759. These earthquakes occurred in the pre-instrumental era, where no seismic data was recorded. Therefore, the ground motion parameters used in the current seismic hazard assessment of the region may be unreliable. Studying the dynamic response of ancient, free-standing structures subjected to ground excitations can serve in identifying the nature of the seismic event that caused damage to these structures. The dynamic response of the multi-drum column at Baalbek and at Iaat was studied numerically using the 3DEC software that is based on the distinct element method. The columns were subjected to various near-fault ground motions to investigate their dynamic behavior and display their mode of collapse. Critical accelerations required for a given period of the near-fault ground excitations were identified. These results show good agreement with those obtained from a simple theoretical block overturning impulse. The results are also used to estimate the magnitude and intensity of historical earthquakes and compare them to previous estimates.

Keywords: Numerical Modeling, Near-fault Ground Excitations, 3DEC, Ground Motion Parameters, Archaeoseismology.

Table of Contents

List of Tables

Table of Figures

Chapter One

Introduction

Major earthquakes destroyed various ancient structures and monuments that are considered a remarkable part of the historical and cultural heritage worldwide. The Mediterranean region is rich with Roman and Greek Temples that are located in high seismicity areas, most are found today as free-standing columns. The fact that some structures have been standing for more than 2500 years although they have been exposed to significant seismic events reveals their ability to withstand destructive earthquakes. This increased the interest of researchers to study the dynamic response of colonnades and free-standing columns to understand the mechanism that allowed their survival during a strong seismic activity. Understanding the dynamic response of such structures is necessary for assessing their seismic vulnerability and establishing ways for strengthening and preserving them. Moreover, it serves in identifying from an archeoseismological perspective the nature of the event that caused the partial or total collapse of these structures. A detailed seismic analysis may reveal some information about previous earthquakes that had hit the region in the study. It helps in estimating different seismic parameters such as the period and the peak ground acceleration that brought the structure to its current deformed position (Galadini et al., 2006; Sintubin, 2011).

In fact, future seismic events will cause additional damage to the historical sites that are located in an active seismic zone such as Greece, Italy, Turkey, and Lebanon. Lebanon is a country rich in heritage sites located in several cities such as Baalbek, Byblos, Tripoli, Saida, and Tyr. Baalbek is located in the Bekaa Valley between the two active faults (Yammouneh and Serghaya) that generated the major historical earthquakes (years 1202 and 1759) and lead to the collapse of most of the columns in the colonnades of Baalbek (only 6 out of 54 columns are remaining from the Temple of Jupiter) (Ambraseys & Barazangi, 1989). Similarly, a not well-known Corinthian column is standing alone in a land in Iaat, 6 km to the northern west of Baalbek ruins. Little information is available on

this column, but what we are certain of is that it has been exposed to the huge earthquakes that caused damage in the Bekaa Valley. The absence of the seismic records of the major earthquake events that hit the Bekaa Valley requires a multidisciplinary approach to investigate the ground motion parameters. This could be achieved by analyzing the seismic response of the ancient structures that were exposed to these historical earthquakes.

Chapter Two

Literature review

2.1 Seismicity of Lebanon

The eastern Mediterranean zone is recognized for its seismic quiescence during the last century (instrumental era). In fact, many large earthquakes have occurred along the Dead Sea Transform Fault in the past few centuries (pre-instrumental era). The DSTF is the continental boundary that separates the African plate (west) from the Arabian plate (east). The 1000 km DSTF is shown in Figure 1a, it extends from the top of the Gulf of Aqaba in the south to the south-east of Turkey (Karasu Valley) where it merges with the East Anatolian Fault in the north.

The 170 km Lebanese Restraining Bend (LRB) is a complex faulting system that lies in the DSTF (Figure 1b). It constitutes of the main Yammouneh fault that connects the northern and southern parts of the DSTF, the Rachaya and Serghaya faults that are two parallel faults along the Anti-Lebanon range, and the Roum Fault that branches from the Yammouneh fault along the south-west of Mount Lebanon range (Nemer et al., 2008).

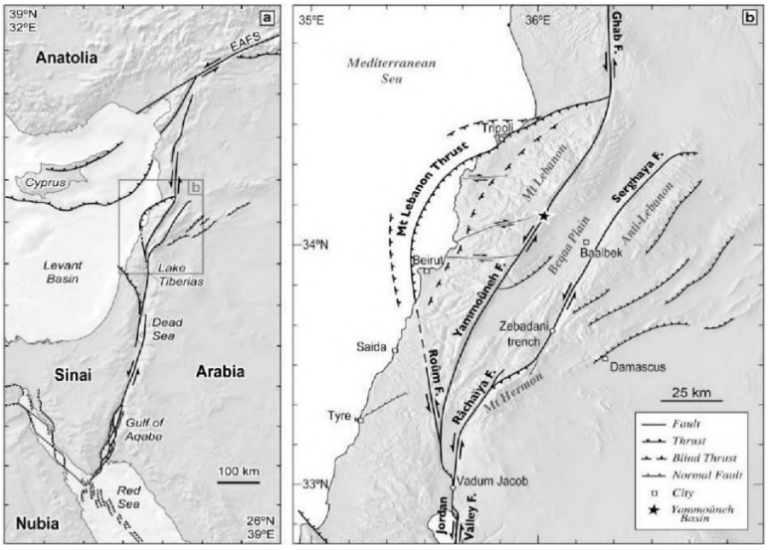

Figure 1: (a) Map of the Dead Sea Transform Fault System (b) Map of the Lebanese Restraining Bend faults (Daëron et al., 2007).

A quite large number of recent and historical earthquakes have occurred in the Eastern Mediterranean region and were all mentioned and classified according to their dates, magnitudes, and locations by Ben-Menahem (1991) and Ambraseys & Jackson (1998). Recently, an updated earthquake catalog for the DSTF was created by Grigoratos et al. (2020) that can be used for seismic hazard assessment. This research focuses on the seismicity of the LRB, especially the major earthquakes that caused destructions in the Bekaa Valley and the nearby areas. The major earthquakes that hit the Bekaa Valley occurred in 551, 991, 1157, 1170, 1202, and the last destructive earthquake in the region was in 1759 (Ben-Menahem, 1991; Ambraseys & Jackson, 1998; Khair et al., 2000; Huijer et al., 2016).

A large earthquake was felt in the Middle East on 20 May 1202 with a magnitude of 7.6 and 33.7°N 35.9°E epicenter. The earthquake caused a remarkable damage in various places in Lebanon, especially in Baalbek with MSK intensity of IX (Ambraseys & Melville, 1988). Different studies have shown that the Yammouneh fault is the source of the 1202 earthquake. (Ambraseys & Barazangi, 1989; Daëron et al., 2007; Wechsler et al., 2014).

The subsequent huge earthquake was in 1759. Ambraseys & Barazangi (1989) described this earthquake by a sequence of two shocks, the first with a 6.6 magnitude 33.1°N 35.6°S epicenter on 30 October followed by a larger event on 25 November (Ms 7.4) and 33.7°N 35.9°S epicenter. A severe damage was caused in the Bekaa Valley with MSK intensity of VIII. The main source of the 1759 earthquake is the Rachaya-Serghaya fault (Gomez et al., 2001; Nemer et al., 2008). The relatively large earthquake required additional investigations which showed evidence of rupture along the Yammouneh fault. (Ambraseys & Barazangi, 1989; Ellenblum et al., 1998; Gomez et al., 2003; Daëron et al., 2007).

Despite the fact that the Yammouneh and Serghaya faults have remained locked and have not generated huge earthquakes during the instrumental era, the faults are active and capable of generating large earthquakes similar to the previous ones (Gomez et al., 2003; Nemer et al., 2008). Therefore, we must be prepared for the occurrence of a major

destructive earthquake and take it into consideration for the assessment of the seismic hazards in the region.

2.2 Response of multi-drum columns

Classical ancient columns are composed of stone blocks fitted perfectly over each other without mortar and usually a capital is placed at the top. Despite their simple structure, the seismic response of the multi-drum columns is complex and non-linear. The first attempt to study the response of rigid bodies was investigated analytically in 2D on a single rigid block by Housner (1963), who appraised the minimum required horizontal acceleration at the base to overturn the rigid block by applying a half-sine pulse. Later, Makris & Roussos (2000) derived an expression that gives the corrected minimum acceleration needed to overturn a rigid block under near-source ground motion. Koh & Mustafa (1990) performed the first 3D numerical integration on a rigid cylinder, they observed three types of response: rocking, wobbling, and toppling. The wobbling response was found to dominate the rocking response, this conclusion was drawn by Stefanou et al. (2010) who studied analytically and numerically the dynamic motion of a conical frustum. Recently, Vassiliou et al. (2017) developed the simplest 3D extension of Housner's 2D rocking model. The different attempts to study the response of rigid bodies analytically have dealt with simple structures, dynamic response becomes more complicated with multi-drum columns. Therefore, it's practically impossible to study the response of multi-drum columns from an analytical approach as each mode of vibration is governed by an equation of motion.

On the other hand, some researchers analyzed the dynamic response of single and multi-drum columns by performing experiments on scaled models of monuments. Krstevska (1996) studied experimentally the dynamic response of the Colonna Antonina in Rome. Also, Mouzakis et al. (2002) performed a series of experiments to investigate the seismic response of a column of the Parthenon of Acropolis. More recently, Drosos et al. (2014, 2015) carried out an experimental program on scaled multi-drum columns of the Temple of Bassae, the columns were subjected to real seismic records and Richer wavelets that represent intense ground motions. Although the experimental approach may reveal

significant information about the column behavior under seismic excitation, it is very sensitive to minor changes and initial conditions.

Numerical solutions were adopted to overcome the difficulties of the analytical and experimental modeling. The Distinct Element Method (DEM) is one of the numerical solutions used to describe the mechanical behavior of discrete bodies. Psycharis et al. (2000) used the 2D software UDEC (Universal Distinct Element Code) to simulate the response of multi-drum columns found at the Temple of Zeus and the Temple of Apollo. They applied harmonic excitations and earthquake ground motions to the columns and determined the existence a safe-unsafe boundary in the acceleration-period domain. Moreover, Konstantinidis & Makris (2005) used Working Model 2D software to study the sliding movement of the blocks in a multi-drum column. The major finding was that sliding between drums may occur even when the coefficient of friction is greater than the g-value of the ground acceleration. Dimitri et al. (2011) investigated the seismic behavior of multi-drum columns and buttresses under harmonic and step impulses. They presented a detailed examination on the modes of collapse and failure domains of the columns. Sarhosis et al. (2019) used UDEC to investigate the response of monolithic and multi-drum columns when subjected to combined horizontal and vertical excitations. It was observed that the column was more prone to collapse when the harmonic excitation was applied in both directions. Tabbara & Karam (2019) verified the efficiency of the 2D DEM in simulating the dynamic response of multi-drum columns by performing an experimental program on scaled models of Baalbek columns and comparing the results to the 2D UDEC numerical software. They investigated experimentally and numerically the rocking and overturning modes of multi-drum columns under harmonic excitations. The 2D analyses is a time-efficient method that can be used to capture the overall behavior of the columns. However, it may be inaccurate in some cases since it neglects the out-plane movements that the drums undergo even when subjected to in-plane ground excitation.

The three-dimensional distinct element method was adopted to highlight the real dynamic response of classical columns. Papantonopoulos et al. (2002) verified the efficiency of 3DEM by comparing the results of 3DEC (three-dimensional distinct element code) to the results of the experiments performed on a multi-drum column subjected to different real

earthquake motions. Toumbakari & Psycharis (2010) investigated the effect of joint stiffness, friction coefficient, and damping coefficient on the response of the multi-drum column using 3DEC simulation. Stefanou et al. (2011) defined wobbling by the smooth rolling of the drum on its edges with small inclination angles while rocking by the in-plane movement of the drum from one corner to the other. Foti & Vacca (2017) studied the effect of scale and slenderness of a multi-drum column under harmonic pulses using 3DEC. The dynamic response and mode of collapse of the multi-drum columns of Baalbek under various idealized pulses were investigated using 3DEC simulation by Tabbara et al. (2021). The results were compared with those obtained from UDEC and previous experiments; the 3D DEM analysis was proved to be more conservative.

The major observations of the dynamic response of the multi-drum column subjected to ground excitation are (a) Three types of response are observed by the drums during an earthquake motion (rocking, wobbling, and sliding). When the seismic motion is governed by a short period (high frequency), sliding occurs and rocking is limited. On the other hand, when a long period (low frequency) is predominant, the rocking motion is dominant without sliding. As the frequency of the excitation decreases, wobbling is observed (Dimitri et al., 2011; Drosos et al., 2015; Mouzakis et al., 2002). (b) The column response is affected by little changes; each parameter may influence the dynamic behavior. (i) As the friction coefficient of the drum interfaces decreases, the sliding phenomenon increases, and rocking becomes limited. However, when the friction coefficient increases, excessive rocking is observed with limited sliding which might affect the stability of the column (Komodromos et al., 2008; Pitilakis et al., 2017). (ii) The damping coefficient seems to have little effect on the dynamic response, the studies proved that during the seismic excitation changing the value of damping gives approximately the same results. However, the effect of varying damping coefficient may be observed toward the end of the excitation (free vibration) (Papadopoulos et al., 2019; Papantonopoulos et al., 2002). (c) The column response is known as size dependent. Studies showed that slender columns are more prone to collapse. It is worth mentioning columns having the same slenderness but with a larger scale showed higher resistance to collapse than columns with smaller scale (Foti & Vacca, 2017; Papadopoulos et al., 2019).

2.3 Archaeoseismology

Over recent decades, archaeoseismology has been linked to investigations related to the effect of seismic activities on ancient structures. The analysis of archeological structures located across an active fault and affected by past earthquakes has been used to reveal some information about seismic activities that have not been instrumentally recorded. The ancient structures should first be examined for any rupture, ruined blocks, or evidence of collapse to define the nature of the event that brought the structure to its current position. Moreover, this approach may provide quantitative seismic parameters such as the magnitude and the peak ground acceleration of the earthquake. The Levant fault contains many archeological sites that exhibit traces of damage caused by historical earthquakes. Recently, Schweppe et al. (2021) used DEM to determine the slip velocity of the 1202 and 1759 earthquakes by analyzing the deformation caused by these earthquakes on the Crusader fortress at Tel Ateret in the Jordan Gorge. In this study, the ancient columns of Baalbek and Iaat located in the Bekaa valley in Lebanon will be used to determine the key parameters of the seismic activities that hit the Bekaa valley.

2.4 Columns of Baalbek and Iaat

The temple of Jupiter in Baalbek was the most important temples in Ancient Rome, and it has been classified as a UNESCO World Heritage site since1984. The construction of the temple started around 16 BC and nearly complete by about AD 60. It was the largest temple dedicated to Jupiter, as it consisted of a colonnade made up of 54 Corinthian multi-drum columns supporting a layered lintel structure. Each column is 20m in height divided into three cylindrical drums. The blocks were made of a strong yellow limestone quarried locally in Baalbek.

The temple of Jupiter is located between two active faults along the Dead Sea Transform Fault System, 20km to the right of Yammouneh fault (source of 1202 earthquake) and 6km to the left of Serghaya fault (source of 1759 earthquake) (Figure 3a). Most of the columns in the colonnade were overturned after successive near-fault earthquakes, where only 6 columns are remaining today (Figure 2a).

(a) (b)

Figure 2: Real picture of the columns (a) Baalbek (b) Iaat.

The column of Iaat is a Corinthian free-standing column located in Iaat, a town in the Bekaa Valley. Iaat column 8.22km to the north-west of Baalbek (Figure 3b) and is located approximately in the middle between Yammouneh fault and Serghaya fault (Figure 3a), with the following coordinated 34.07°N 36.15°E. The column is 17m in height installed on four plates at the base, it consists of 14 similar drums of calcareous rocks and a capital as shown in Figure 2a. There is no specific date mentioned for the construction of this column, but it probably dates to Roman times. Once a plaque was placed on the northern side of this monument. Unfortunately, it has been removed a long time ago.

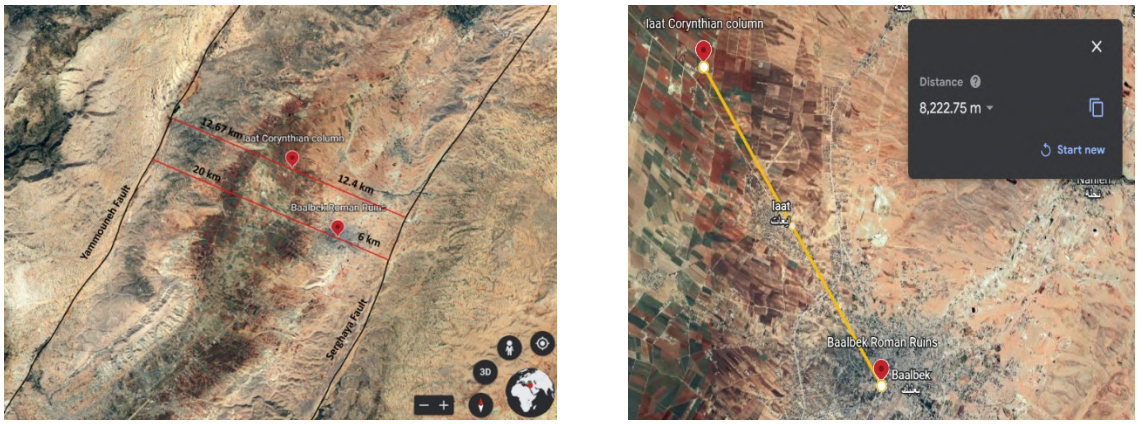

Figure 3: (a) Map showing the location of the columns with respect to the Yammouneh and Seghaya faults. (b) Map showing the distance between Ruins of Baalbek and Iaat column.

Iaat column has been devastated by the major destructive earthquakes that hit the Bekaa Valley and caused destruction to Baalbek colonnades. Some drums of Iaat column are damaged at their edges probably due to the rocking phenomenon. Normal stresses are concentrated near the edges of the blocks due to rocking during the seismic excitation, that's why these locations are found to be damaged as observed by Pitilakis et al. (2017). The flexible base of this column may be one of the reasons for its high resistivity to ground motion. An experimental study was performed by Foti & Vacca (2017) to investigate the influence of deformable foundations on the dynamic response of the multi-drum column. It was proven that the deformable foundation improves the stability of the column as it acts in an elastic behavior.

The dynamic behavior of multi-drum columns has been studied extensively in the literature; various types of ground motion were applied to multi-drum columns to predict their dynamic response. The aim of this research is to perform a detailed analysis on the response of the Baalbek and Iaat columns when subjected to ground excitations to characterize the earthquakes that hit the Bekaa Valley and estimate the magnitude and acceleration. Simplified near-field ground motion pulses were applied to the columns with different combinations of period and acceleration.

Chapter Three

Methodology

3.1 Research Aim and Objectives

The aim of this research is to study the dynamic response of Baalbek and Iaat columns when subjected to near fault ground excitations and earthquake records to estimate some characteristics of historical earthquakes.

The objectives are:

1. Survey existing literature on the seismic behavior of multi-drum columns.
2. Choose the suitable input parameters for the numerical model to conduct the research.
3. Choose the ground excitations that will be applied to the model (near-fault ground excitations).
4. Start by analyzing the seismic response of the column when subjected to simple regular pulses.
5. Establish quantitative and qualitative criteria to identify the dominant pulse in the near-fault earthquake.
6. Use the results to investigate the column's response due to earthquake records.
7. Analyze the results to estimate the critical combinations of periods and accelerations of the previous earthquakes.

3.2 Research Significance

Lebanon has been devastated by major earthquakes with a magnitude greater than 7, the problem is that these earthquakes occurred in the pre-instrumental era where no seismic data was recorded. The faults in Lebanon are active and the period of reoccurrence of these earthquakes is overdue, therefore the absence of the historical data requires the researchers to investigate about their seismic characteristics. This research presents the

first study in Lebanon that deduces the seismic parameters of an earthquake from the dynamic response of ancient structures. The results can be used to estimate the magnitude of the upcoming earthquakes and identify the peak ground acceleration that should be used in the seismic design of structures in Lebanon.

3.3 Numerical Modeling

The distinct element method which was introduced by Cundall in 1971 was adopted to study the response of Iaat column. DEM is based on the concept that the discontinuous medium is represented by an assembly of discrete blocks that interact along contact planes. Where the discontinuities represent the areas of interaction between the blocks. In DEM, the rigid bodies are allowed to undergo finite displacements and rotations, including complete detachment. The dynamic behavior is represented numerically by assuming constant velocities and accelerations during a time step. The time step is chosen so small to prevent the propagation of discontinuities between alternative blocks. The DEM process can be summarized by repeated cycles that begin by calculating the motion of blocks in terms of velocity and acceleration within a time step. Each time step produces new block position with new contact forces, the new contact forces are determined using the force-displacement law. The updated body forces are used to update the velocity and motion of each block with the application of Newton's second law.

The numerical model of Baalbek and Iaat column was developed with the use of the commercial DEM software 3DEC (Itasca Consulting Group Inc, 2019). The efficiency of 3DEC in analyzing the response of multi-drum columns was validated experimentally by different authors (Papantonopoulos et al., 2002; Tabbara et al., 2021). The seismic response of these monuments is very sensitive to geometric changes and input parameters (Drosos et al., 2014). Therefore, the columns were modeled to represent the real scale with accurate geometry and dimensions. The column of Baalbek is 20m high, it consists of three drums with a 2.2m diameter and variable heights of 7.5m, 5.5m, and 4m respectively from the bottom where it is supported by a 1m high base block foundation to the top where a 2m capital is found (Figure 4a). Iaat column is 17m in height and located on four square plates at the base, a cylindrical shape plinth (D=2m and h=60cm) is located above the

base. The plinth supports a torus that is divided into two parts. The column is characterized by fourteen similar drums (D=1.6m and h=85cm) and a capital as shown in Figure 4b.

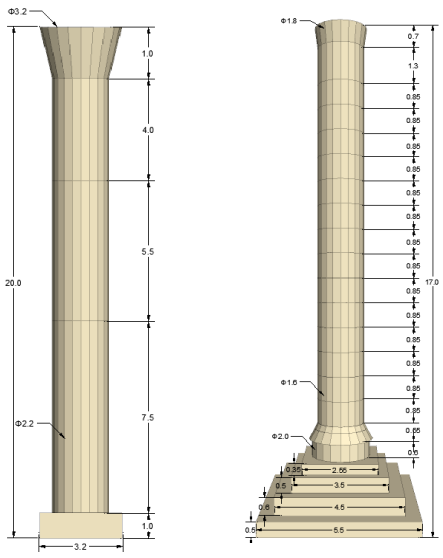

Figure 4: Model of columns with dimensions in meters (a) Baalbek column (b) Iaat column

The DEM blocks were modeled as rigid with no penetration and with a density equal to 2720 kg/m^3. Mohr-Coulomb model was used to assume the joint material, the friction angle = 26° was experimentally determined by Tabbara & Karam (2019) on a reduced model of Baalbek column between limestone blocks. The dilation angle = 0° and both cohesion and tension cutoff are equal to zero. The normal stiffness Kn and the shear stiffness Ks of the blocks were determined experimentally by attaching a spring in each direction. The spring stiffness was set to 200 GPa/m in both directions, this value was obtained by the free rocking experiments on 1m blocks where the block overlap tolerance was limited to 0.05% of the block width (Karam & Tabbara, 2020). As stated in the literature, the damping coefficient value doesn't affect the stability of the columns during strong excitations, the value of damping plays a role during free vibration. Since the analysis of the columns is concerned with the collapse during strong ground excitations, the damping coefficient was set to zero.

Two types of loads will be applied to the model: (i) Self-weight of the blocks and (ii) Simplified near-fault ground excitations. Mavroeidis & Apostolos (2003) proposed a simplified analytical model to represent near-field ground motions that successfully

replicate both qualitatively and quantitatively the recorded time histories of near-fault acceleration, velocity, and displacement. The pulses have the potential to advance the study of elastic and inelastic structures subjected to near-fault seismic excitations. The proposed analytical model of the near-fault ground velocity and acceleration pulses are shown in equations 1 and 2, respectively. The key parameters of the pulses are the period (T_p) that can be calculated by the inverse of the frequency (Equation 3), the parameter that controls the amplitude (A), and the two variables γ and ν. As gamma (γ) increases more oscillations appear in the signal (γ =1,2, and 3 will be used). Nu (ν) affects the shape of the pulse, ν = 0° generates symmetrical velocity pulses with reversed polarities and ν = 90° generates anti-symmetrical velocity pulses (Figure 5). Table 1 shows the values of the peak ground acceleration (A_p) as function of A for different values of γ and ν.

Each column was subjected to six types of idealized pulses with different combinations of period (T_p ranging from 1s to 8s) and acceleration (A_p ranging from 0.15g to 1.0g). A total of 864 simulations for the idealized pulses were performed for each column. In addition to that, the columns were subjected to 40 pulses that represent recorded near-fault ground excitation of real earthquakes. The input parameters for the analytical model of each earthquake are presented in Table 2.

$$v(t) = \frac{A}{2}\left[1 - cos\left(\frac{2\pi fp}{\gamma}t\right)\right] cos[2\pi fpt - \gamma\pi + \nu] \qquad 0 \le t \le \gamma Tp \qquad (1)$$

$$a(t) = \frac{A}{2}\left\{2\pi fp\left[\frac{1}{\gamma}sin\left(\frac{2\pi fp}{\gamma}t\right)\right] cos[2\pi fpt - \gamma\pi + \nu] - \left[1 - cos\left(\frac{2\pi fp}{\gamma}t\right)\right] sin(2\pi fpt - \gamma\pi + \nu)\right\} \qquad (2)$$

$$T_P = \frac{1}{f_p} \qquad (3)$$

γ	ν	Acceleration	Velocity	Displacement
1	0	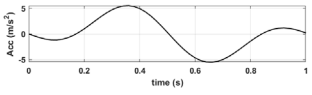	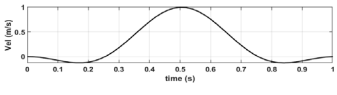	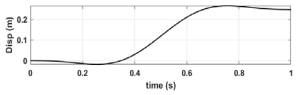
1	90	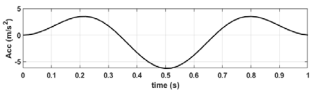	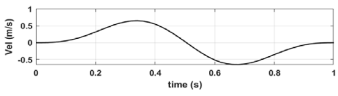	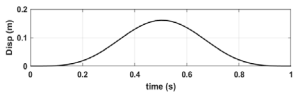
2	0	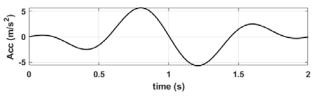	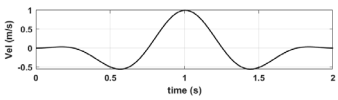	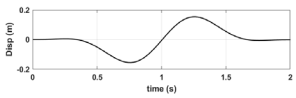

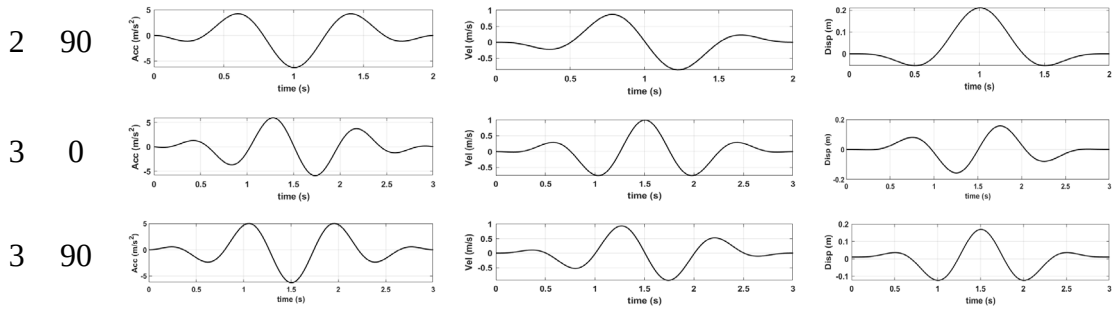

Figure 5: Acceleration, velocity, and displacement time histories as function of γ and ν (A = 1 and fp = 1).

Table 1: Values of Ap as function of A.

γ	1	1	2	2	3	3
ν	0	90	0	90	0	90
Ap	1.76πAfp	2πAfp	1.811πAfp	2πAfp	1.891πAfp	2πAfp

Table 2: Input parameters obtained by fitting the analytical model to recorded near-field ground motions.

No.	Location	Station	Component	A	γ	ν	fp (Hz)
1a	Parkfield, CA, USA	C02	SN	60.0	1.700	100.0	0.500
2a	San Fernando, CA, USA	PCD	SN	115.0	1.600	180.0	0.680
3a	Gazli, USSR	KAR	Rad	45.0	2.900	70.0	0.238
4a	Bucharest, Romania	BRI	SN	62.0	2.400	200.0	0.470
5a	Tabas, Iran	TAB	SP	104.0	2.200	180.0	0.190
6a	Coyote Lake, CA, USA	GA6	SN	48.0	1.550	315.0	1.000
7a	Imperial Valley, CA, USA	E04	SN	71.0	1.900	305.0	0.225
7b	Imperial Valley, CA, USA	E05	SN	84.0	1.900	300.0	0.255
7c	Imperial Valley, CA, USA	E06	SN	96.0	2.100	265.0	0.260
7d	Imperial Valley, CA, USA	E07	SN	79.0	2.100	25.0	0.275
7e	Imperial Valley, CA, USA	EMO	SN	78.0	2.300	0.0	0.340
8a	Mexicali Valley, Mexico	VCT	SN	80.0	1.500	270.0	0.270

9a	Morgan Hill, CA, USA	HAL	SN	38.0	1.750	130.0	1.150
10a	Palm Springs, CA, USA	NPS	SN	60.0	1.700	170.0	0.800
10b	Palm Springs, CA, USA	DSP	SN	21.0	2.000	80.0	0.600
11a	Whittier Narrows, CA, USA	DOW	SN	29.0	2.200	220.0	1.200
11b	Whittier Narrows, CA, USA	NWK	SN	20.0	2.100	200.0	1.350
12a	Superstition Hills, CA, USA	PTS	SN	112.0	1.800	237.0	0.445
12b	Superstition Hills, CA, USA	ELC	SN	46.0	1.650	210.0	0.430
13a	Loma Prieta, CA, USA	LGP	SN	60.0	3.000	280.0	0.310
13b	Loma Prieta, CA, USA	STG	SN	47.0	1.900	150.0	0.270
14a	Sierra Madre, CA, USA	COG	Rad (filt)	9.2	2.300	260.0	1.100
15a	Erzincan, Turkey	ERZ	SN	67.0	2.500	210.0	0.410
16a	Landers, CA, USA	LUC	SN	100.0	1.210	55.0	0.170
17a	Northridge, CA, USA	JFA	SN	87.0	2.300	100.0	0.330
17b	Northridge, CA, USA	RRS	SN	142.0	1.700	20.0	0.800
17c	Northridge, CA, USA	SCG	SN	93.0	2.500	0.0	0.340
17d	Northridge, CA, USA	SCH	SN	80.0	2.300	0.0	0.330
17e	Northridge, CA, USA	NWS	SN	94.0	1.700	200.0	0.370
18a	Aigion, Greece	AEG	Long	44.5	1.450	75.0	1.400
18b	Aigion, Greece	AEG	Tran	61.0	1.200	205.0	1.480
19a	Izmit, Turkey	ARC	SN	41.0	1.380	225.0	0.140
19b	Izmit, Turkey	SKR	SP	67.0	1.023	5.0	0.105
19c	Izmit, Turkey	YPT1	SP (first pulse)	35.0	1.550	90.0	0.190
19d	Izmit, Turkey	YPT2	SP (second pulse)	91.5	1.050	10.0	0.137
19e	Izmit, Turkey	GBZ	SN	34.5	2.200	220.0	0.210
19f	Izmit, Turkey	GBZ	SP	28.0	1.800	85.0	0.165
20a	Chi-Chi, Taiwan	TCU052	SN	225.0	1.048	190.0	0.079
20b	Chi-Chi, Taiwan	TCU068	SN	332.0	1.055	190.0	0.082

20c	Chi-Chi, Taiwan	TCU075	SN	105.0	1.200	220.0	0.170
20d	Chi-Chi, Taiwan	TCU076	SN	70.0	1.088	200.0	0.175
20e	Chi-Chi, Taiwan	TCU129	SN	52.0	1.090	200.0	0.130

A detailed investigation on the response of the single columns to the near-faults ground excitations was performed showing the critical combinations of periods and accelerations that cause the overturning of the blocks. Moreover, the mode of collapse (Total or partial) and the movement of the blocks (in-plane or out of plane) were tracked. This approach is based on the concept that the earthquake records can be treated as a series of pulses when analyzing the response of rocking blocks. Therefore, it is proposed to develop a modeling approach starting with simple pulses, and then using the results to analyze real seismic records (Housner, 1963; Karam & Tabbara, 2020). The detailed seismic investigation of Baalbek and Iaat columns contributes to archaeoseismology to determine some parameters of earthquakes that previously hit the region based on their impact on the monument.

3.4 Theoretical modeling

Tabbara & Karam (2019) developed an analytical model for the overturning of a rigid block under a specific pulse as a function of the period of the signal, size of the block, and the applied acceleration along the horizonal axis. The theoretical model is based on the concept that when the rotational angle of the block θ exceeds the limit value α which is the critical stability angle, the block is about to overturn. The static equilibrium between the overturning moment and the restoring moment shows that for the rocking motion to start, the horizontal acceleration caused by the applied pulse (a) must reach at some point the minimum value αg:

$$a \geq \alpha g \qquad (4)$$

The friction coefficient (μ) is assumed high enough to permit rocking without sliding. Therefore, for the block to overturn, it must lift its center of gravity by rotating around the corners until it reaches an unstable position.

The equation required to plot the critical impulse curve is as follows:

$$\frac{a_p}{\alpha g} = \frac{1}{p\beta t_p} \quad (5)$$

Where, a_p is the peak acceleration of the maximum area under the pulse, t_p is its duration, and β is the fullness factor calculated as per equation 7. For a given block of height 2h and width 2b, the frequency parameter is $p = \sqrt{\frac{3g}{4R}}$ where $R = \sqrt{h^2 + b^2}$ and g is the gravitational acceleration. The height of the columns was taken excluding the base because the collapse of the columns was observed starting from the first drum. For Baalbek column, height (2h = 19m) and width (2b = 2.2m). For Iaat column, height (2h = 13.9m) and width (2b = 1.6m). Therefore, the critical stability angle ($\alpha = \tan^{-1}(b/h)$) is equal to 0.1153 and 0.1146 for Baalbek and Iaat columns, respectively.

The transition point that is intersection point between the two equations (4 and 5) can be calculated as follows:

$$\bar{t_p} = \frac{1}{p\beta} \quad (6)$$

For any pulse:

$$\beta\, t_p\, a_p = \int_0^{t_p} a(t)dt \quad (7)$$

The area under the curve of each pulse was calculated to determine the value of the fullness factor (β) (Table 3). The difference between Tp which is the actual period of the pulse and tp which is the duration of the maximum impulse is clarified in Figure 6.

Table 3: Values of fullness factor (β) and tp/Tp ratio for the 6 near fault ground motion pulses.

γ	1	1	2	2	3	3
ν	0	90	0	90	0	90
β	0.6099	0.6206	0.6225	0.6255	0.6268	0.6309
tp/Tp	0.3335	0.3333	0.4381	0.4431	0.4718	0.4735

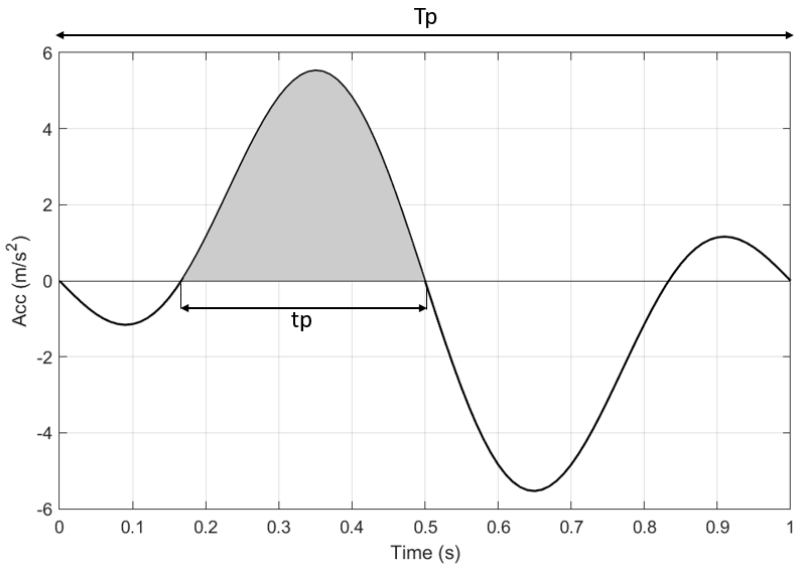

Figure 6: Acceleration pulse of the near-fault ground excitations showing the difference between Tp and tp.

Chapter Four

Results and Discussion

4.1 Dynamic response of Baalbek and Iaat columns using numerical modeling

The columns of Baalbek and Iaat were each subjected to different near-fault ground excitations. The pulses used in the dynamic analysis were generated using an analytical model developed by Mavroeidis & Apostolos (2003). The seismic response of each column was investigated under six pulses generated by the analytical model, with three values for gamma (γ = 1, 2, and 3) and v set to 0° or 90°. The values of gamma and nu were chosen to produce near-fault ground excitations with different numbers of oscillations and impulse characteristics. This was done to generate pulses with varying characteristics capable of simulating as many as possible of the near-source acceleration, velocity, and displacement time histories. Each column was subjected to the near-fault ground motions with different combinations of period (ranging from 0.1s to 8s) and acceleration (ranging from 0.05g to 1.0g). The numerical modeling results were obtained using 3DEC simulations; Tables 4 and 5 show the modes of collapse of the Baalbek under near-fault ground excitations with γ = 1 and v = 0° and γ = 1 and v =90°, respectively. Tables 6 and 7 show the modes of collapse of the Iaat column under near-fault ground excitations with γ = 1 and v = 0° and γ = 1 and v =90°, respectively A snapshot of the side and the top view is provided at the moment of collapse of the columns. The side view displays the mode of collapse of the columns (total or partial), the number of overturning blocks, and the position of the surviving blocks. The top view indicates whether the collapse is in-plane or out-of-plane. The out-of-plane movement shows evidence of wobbling.

The results of the numerical modeling were summarized in multiple charts, each data point represents a single simulation of the column under a near-field ground motion with a specific period and acceleration. Figures 7 and 8 show the modes of collapse of Baalbek

and Iaat columns when subjected to various near-fault ground excitations, respectively. A green color indicates that the column did not collapse at the end of the applied pulse. When the column undergoes collapse before the end of the applied pulse, it is represented by a red color.

Global response of Baalbek columns under idealized near-fault ground excitations:

- At large periods, greater than 4s, total collapse of the column was observed for all pulses. The column exhibits two modes of collapse, the first is the one shown in Table 4 for near-fault ground excitations with (γ=1 and ν=0°) in which the column loses its stability and overturns from the first drum. The second is as shown in Table 5 for near-fault ground excitations with (γ=1 and ν=90°), where rocking is observed prior to overturning. Wobbling intervenes and causes the out-of-plane collapse of the column. Wobbling was most visible for columns under near-fault ground excitations with ν=90°. Therefore, the collapse mode of the column is affected by the shape of the pulse applied. The first mode of collapse is similar to the one observed by Tabbara et al. (2021) for Baalbek column subjected to 25 cycles of periodic pulses.
- At intermediate periods, between 1.5s to 3s, total and partial collapse of the column is observed for most of the near-fault ground excitations applied. Rocking is observed along with wobbling causing the column to collapse out of plane. The wobbling phenomenon, which causes the drum to roll around its edges, is most common for near-fault ground motions having ν=90°. The acceleration required to cause the collapse of the column is smaller for shorter periods. The column response at intermediate periods for near-fault ground excitations is similar to the response of the column observed under 25 cycles of periodic signals, where wobbling was observed prior to overturning (Tabbara et al., 2021).
- At small period, less than 1s, the column survived for all pulses. For periods equals to 0.8s and 1s with high acceleration values, rocking and wobbling is observed at the top of the column. At lower periods, the pulses have no effect on the column. Similar observations were observed by Tabbara et al. (2021). However, one or

more drums topple from the top of the column under the 25 cycles of periodic pulse.

It is worth noting that the period and acceleration values required to collapse the Baalbek column under near-fault ground excitations are greater than those required to collapse the column under 25-cycle periodic pulses.

Global response of Iaat columns under idealized near-fault ground excitations:

- At large periods, greater than 4s, total and partial collapse of the column is observed. At Tp= 7s and 8s, the column loses its stability and collapses from the first drum. At smaller periods between 4s and 6s, total collapse is observed for large acceleration values, and partial collapse is observed for smaller ones (refer to Tables 6 and 7 and to Figure 8). No wobbling was observed.
- At intermediate periods, between 1.5s and 3s, partial collapse of the column is observed. Total collapse is observed under near-fault ground pulses with high acceleration values. It is worth noting that for the same period, the column may collapse for lower acceleration values while surviving for higher ones as shown in the charts in Figure 8. The dynamic response of multi-drum columns is dependent on many factors such as the behavior of the drums during ground excitation and the impulse characteristics (period and acceleration). Wobbling was observed for some near-fault ground pulses with ν=90°.
- At small periods, less than 1s, Iaat column survived for all pulses. Rocking occurs at high acceleration values, but the angle of rotation of the blocks is not large enough to cause overturning. Wobbling takes over during rocking, and the drums begin to rotate with a slight inclination around the edges. This results a minor in-plane displacement between the drums at the upper part of the columns. The seismic excitations have no effect on the columns with periods less than 0.4s.

The dynamic response of Baalbek and Iaat columns are similar at some points. At large periods, which are greater than 4s, the columns of Baalbek and Iaat collapsed for acceleration greater and equal to 0.15g for all the chosen pulses. The collapse of the columns is expected for this acceleration value because it is greater than the limit αg

(0.1153g for Baalbek and 0.1146g for Iaat), which indicates the required condition for the inception of rocking. The columns survived all pulses with acceleration values less than αg. Baalbek column shows more wobbling and out-of-plane collapse. The geometry and number of drums in each column may be the reason behind some differences in the mode of collapse of the columns.

Table 4: Mode of collapse of Baalbek column under near-fault ground excitations (γ=1 and ν=0) with different combinations of periods and accelerations (friction angle of 26°) (a) Side view (b) Top view.

Ap \ Tp	0.1	0.4	0.8	1	1.5	2	3	4	5	6	7	8
1.0g	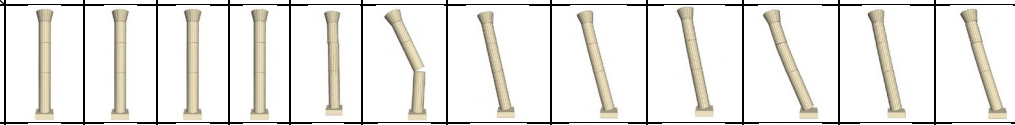											
0.9g	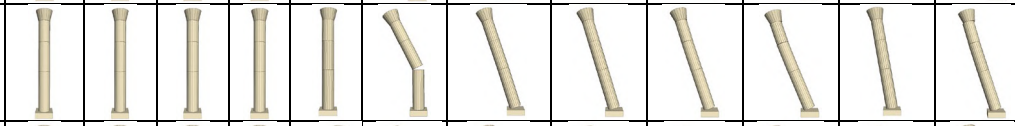											
0.8g												
0.7g	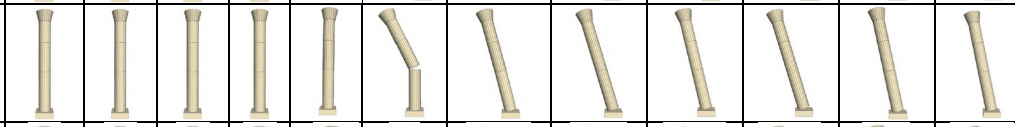											
0.6g	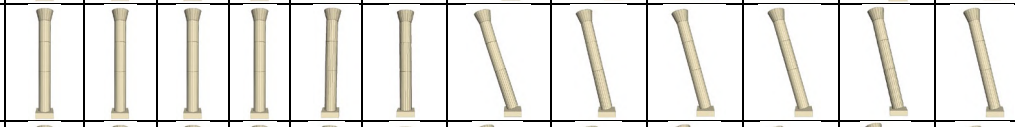											
0.5g	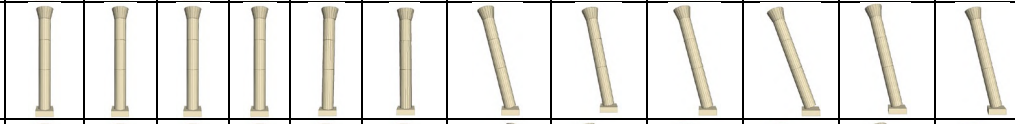											
0.4g												
0.3g	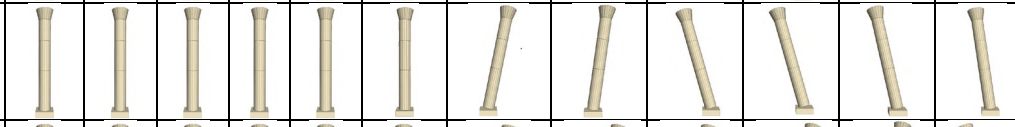											
0.2g	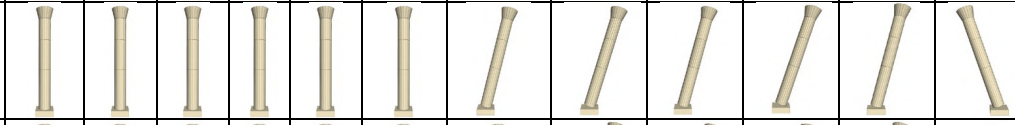											
0.15g	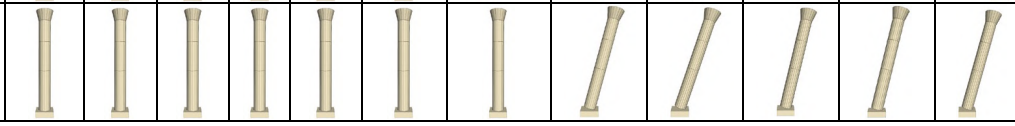											

0.1g	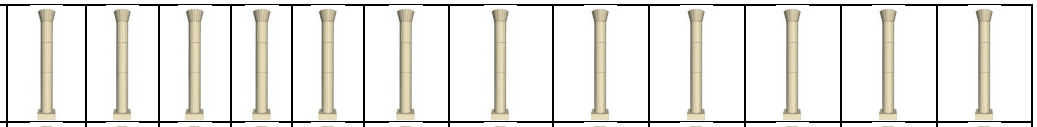											
0.05g	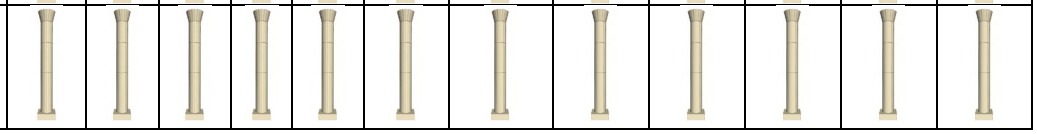											

(a)

Ap \ Tp	0.1	0.4	0.8	1	1.5	2	3	4	5	6	7	8
1.0g												
0.9g	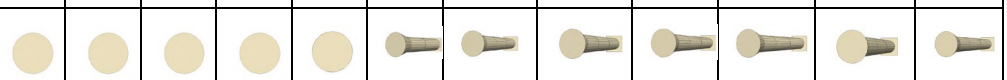											
0.8g												
0.7g	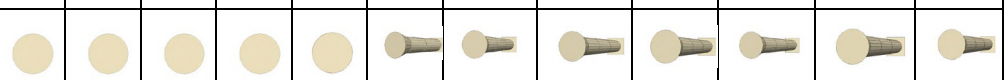											
0.6g												
0.5g												
0.4g												
0.3g												
0.2g												
0.15g	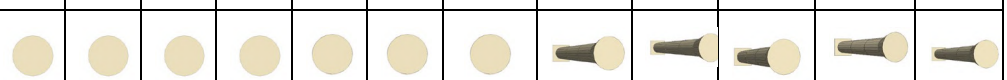											
0.1g	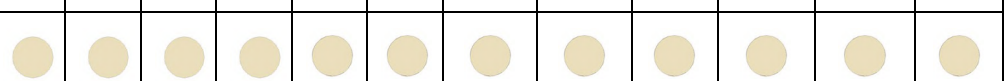											
0.05g	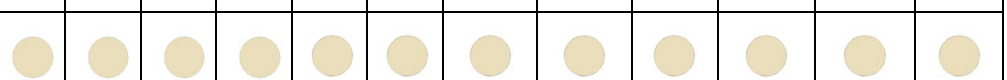											

(b)

Table 5: Mode of collapse of Baalbek column under idealized near-fault ground excitations (γ=1 and ν=90) with different combinations of periods and accelerations (friction angle of 26°) (a) Side view (b) Top view.

Ap \ Tp	0.1	0.4	0.8	1	1.5	2	3	4	5	6	7	8
1.0g	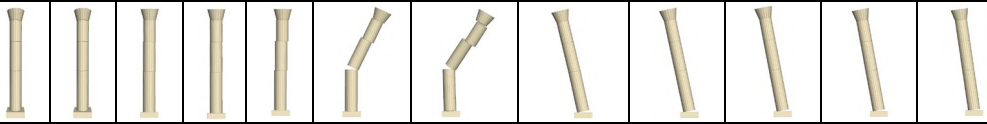											
0.9g	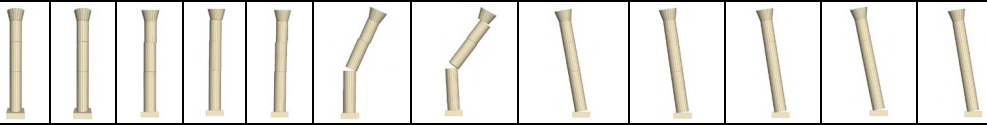											
0.8g	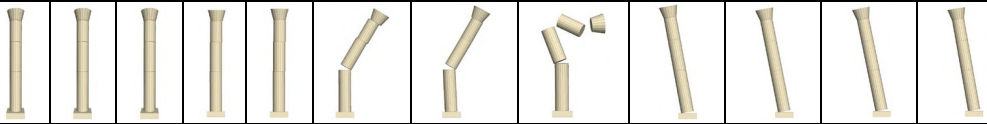											
0.7g	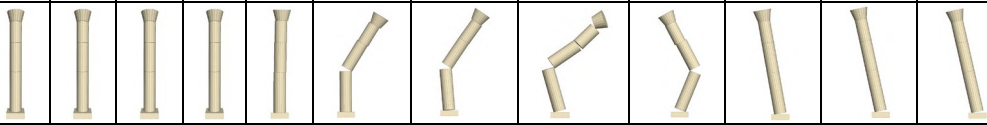											
0.6g	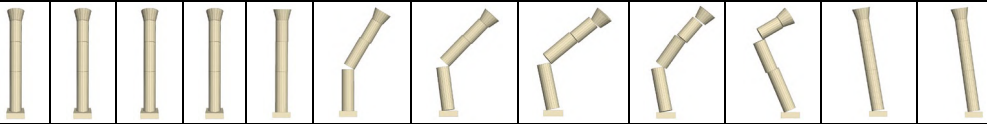											
0.5g	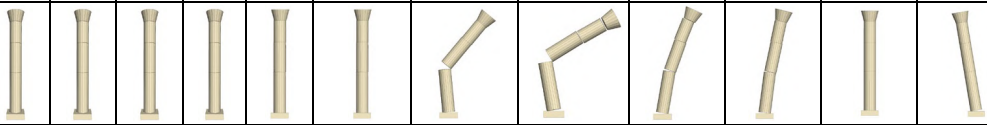											
0.4g	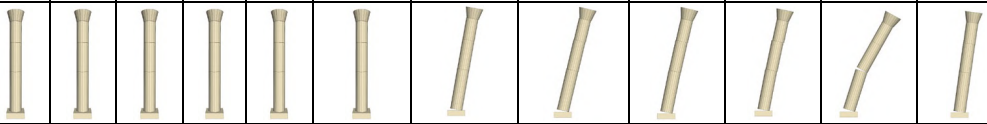											
0.3g	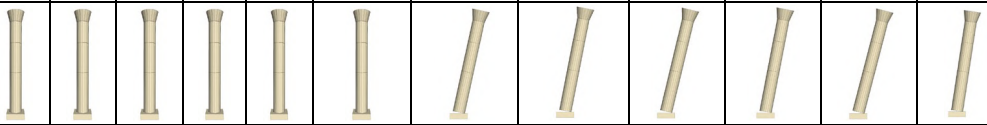											
0.2g	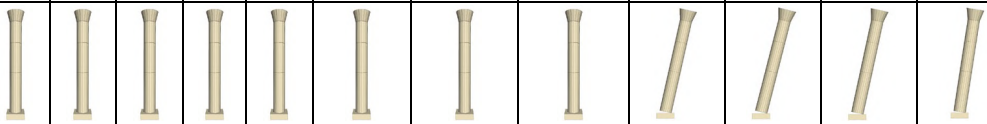											
0.15g	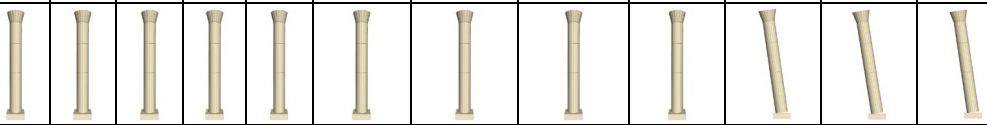											
0.1g	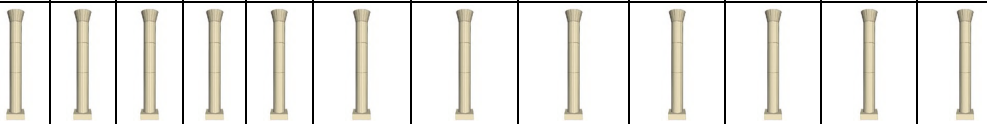											
0.05g	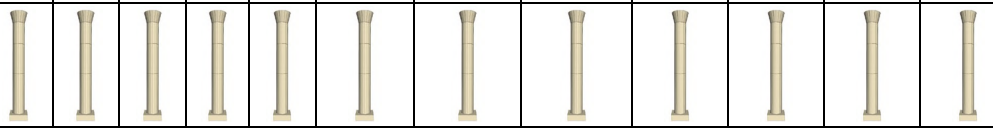											

(a)

Tp / Ap	0.1	0.4	0.8	1	1.5	2	3	4	5	6	7	8
1.0g												
0.9g												
0.8g												
0.7g												
0.6g												
0.5g												
0.4g												
0.3g												
0.2g												
0.15g												
0.1g												
0.05g												

(b)

Table 6: Mode of collapse of Iaat column under idealized near-fault ground excitation (γ=1 and ν=0) with different combinations of periods and accelerations (friction angle of 26°) (a) Side view (b) Top view.

Ap \ Tp	0.1	0.4	0.8	1	1.5	2	3	4	5	6	7	8
1.0g	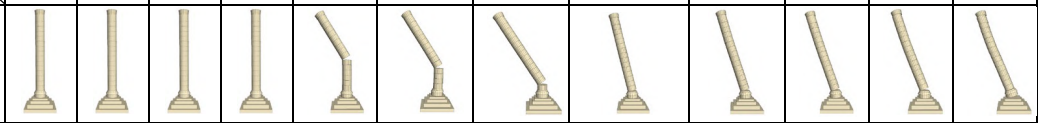											
0.9g	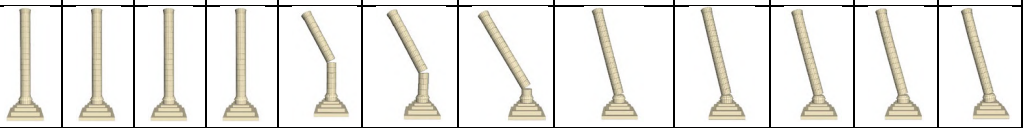											
0.8g	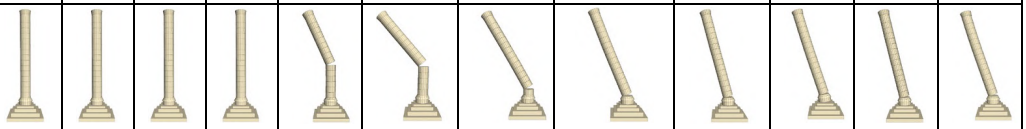											
0.7g	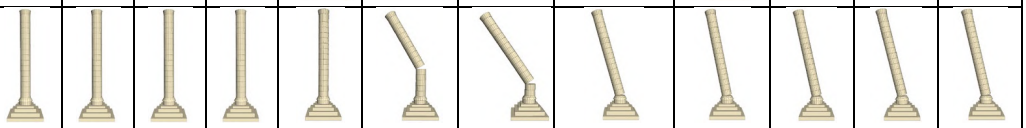											
0.6g	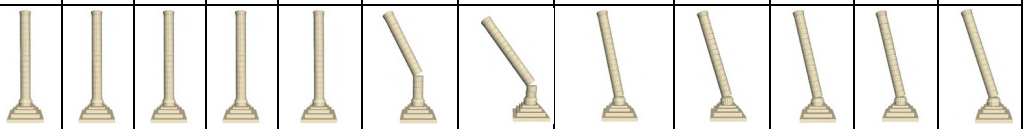											
0.5g	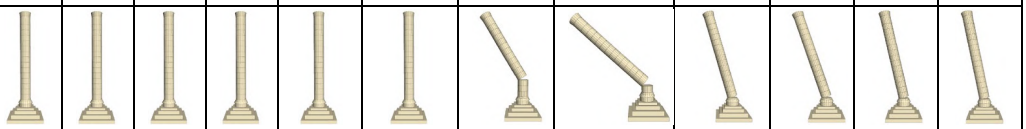											
0.4g	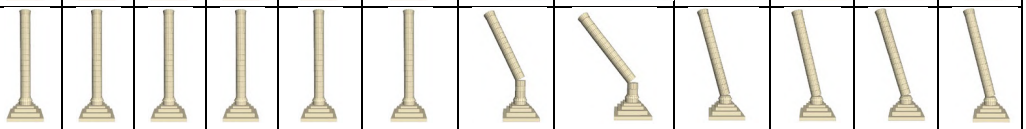											
0.3g	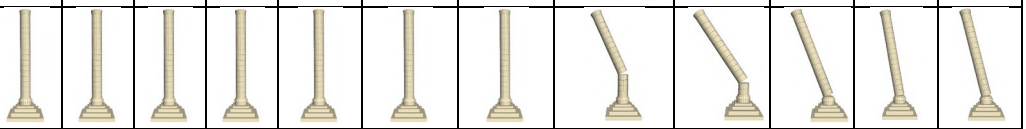											
0.2g	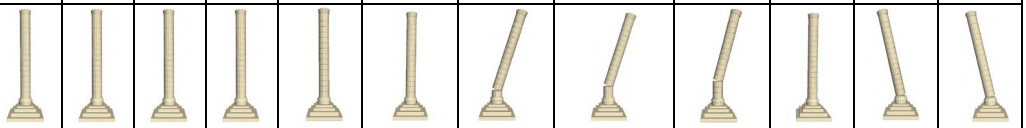											
0.15g	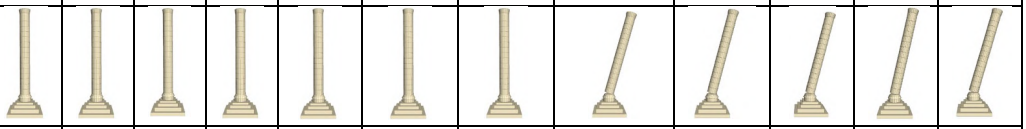											
0.1g	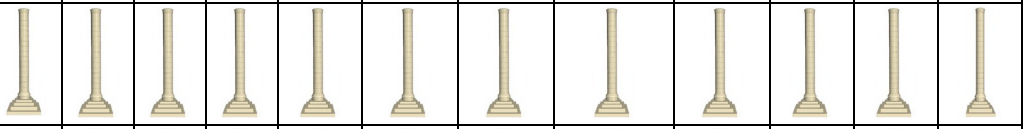											
0.05g	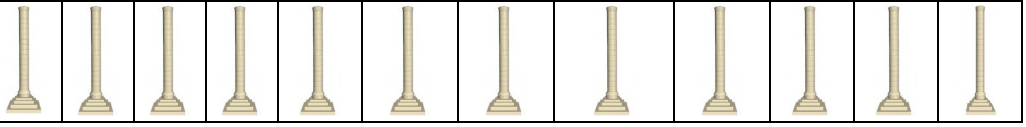											

(a)

Tp / Ap	0.1	0.4	0.8	1	1.5	2	3	4	5	6	7	8
1.0g												
0.9g												
0.8g												
0.7g												
0.6g												
0.5g												
0.4g												
0.3g												
0.2g												
0.15g												
0.1g												
0.05g												

(b)

Table 7: Mode of collapse of Iaat column under idealized near-fault ground excitation (γ=1 and ν=90) with different combinations of periods and accelerations (friction angle of 26°) (a) Side view (b) Top view

Ap \ Tp	0.1	0.4	0.8	1	1.5	2	3	4	5	6	7	8
1.0g	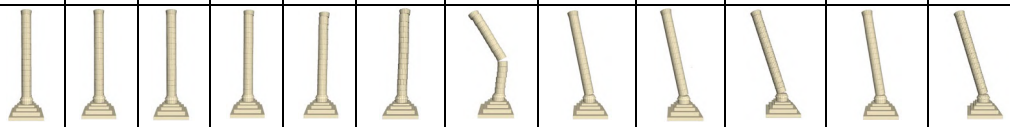											
0.9g	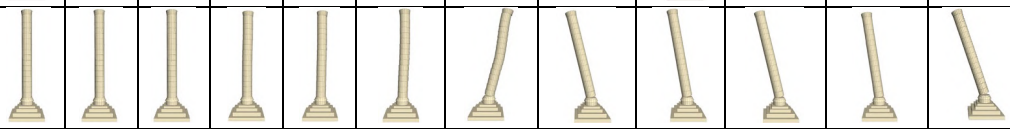											
0.8g	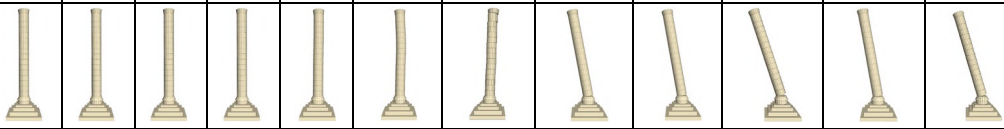											
0.7g	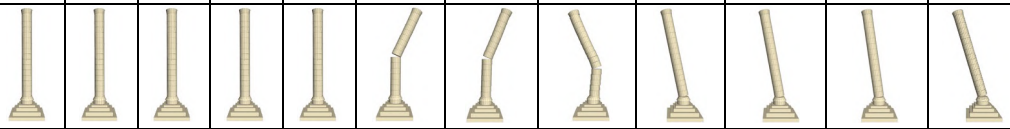											
0.6g	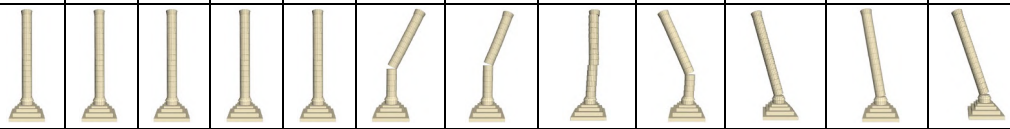											
0.5g	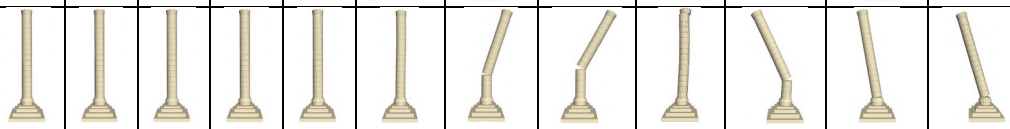											
0.4g	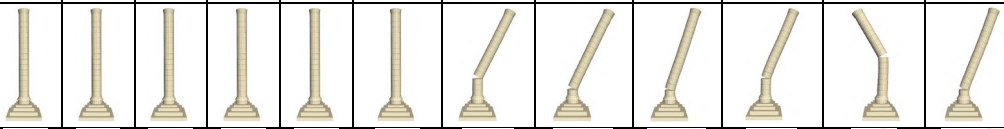											
0.3g	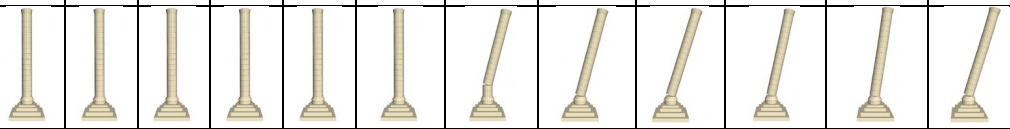											
0.2g	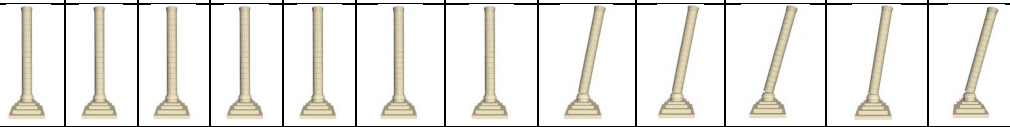											
0.15g	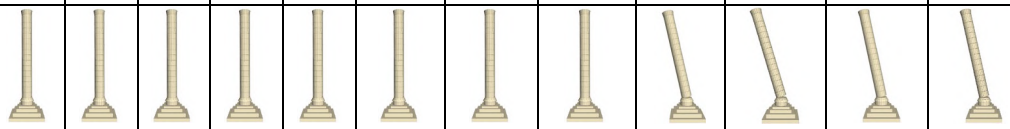											
0.1g	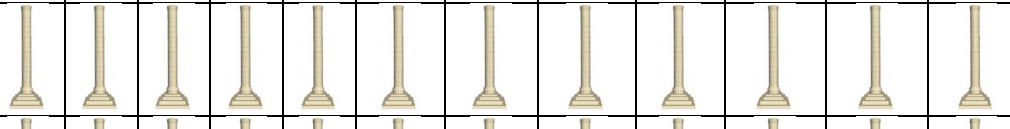											
0.05g	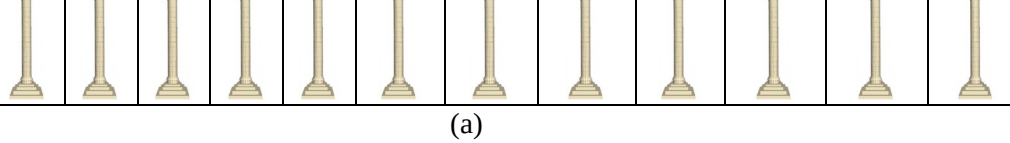											

(a)

Tp / Ap	0.1	0.4	0.8	1	1.5	2	3	4	5	6	7	8
1.0g												
0.9g												
0.8g												
0.7g												
0.6g												
0.5g												
0.4g												
0.3g												
0.2g												
0.15g												
0.1g												
0.05g												

(b)

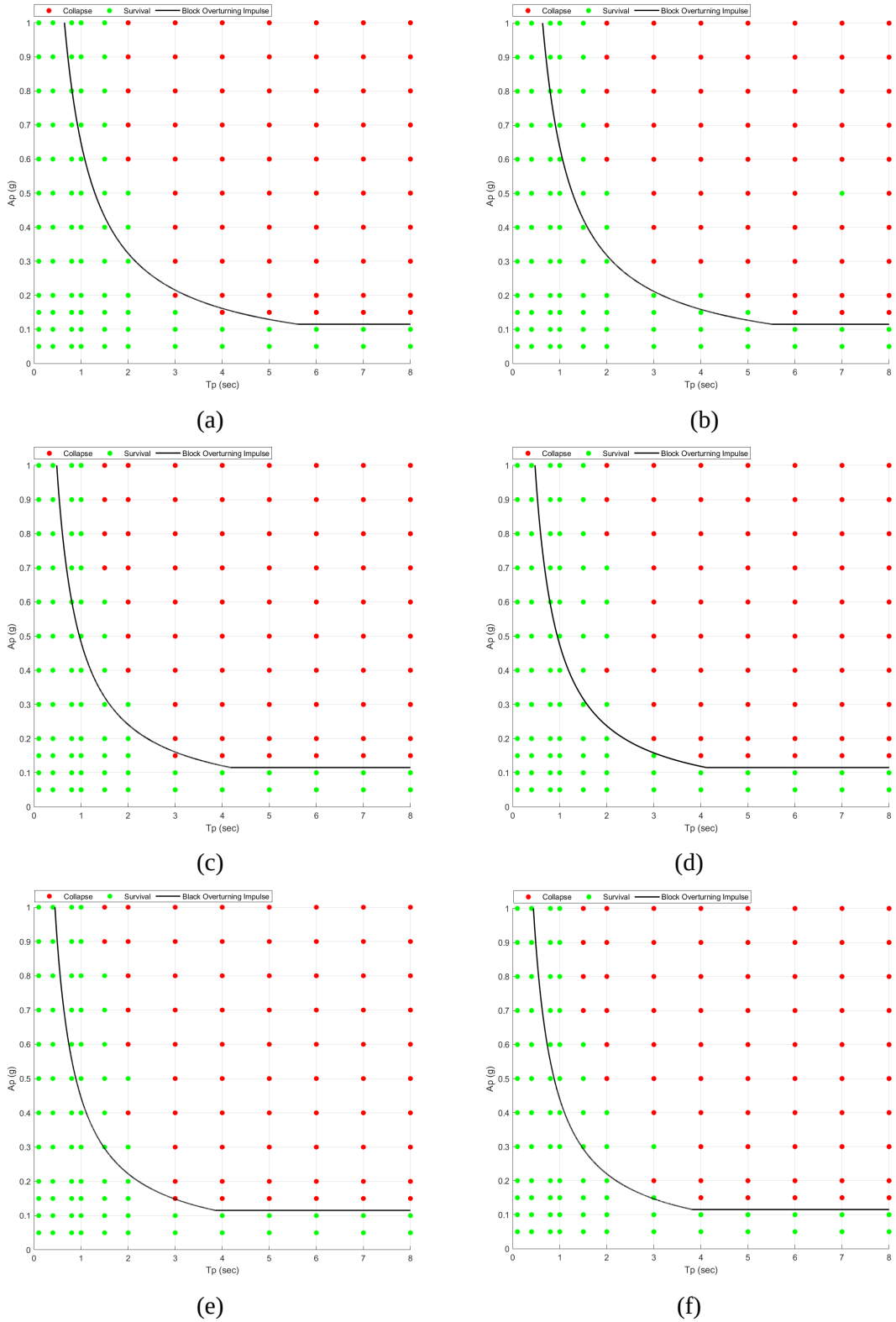

Figure 7: Charts showing stability of Baalbek column under idealized near-fault ground excitation (friction angle of 26°) (a) γ=1 and ν=0 (b) γ=1 and ν=90 (c) γ=2 and ν=0 (d) γ=2 and ν=90 (e) γ=3 and ν=0 (f) γ=3 and ν=90.

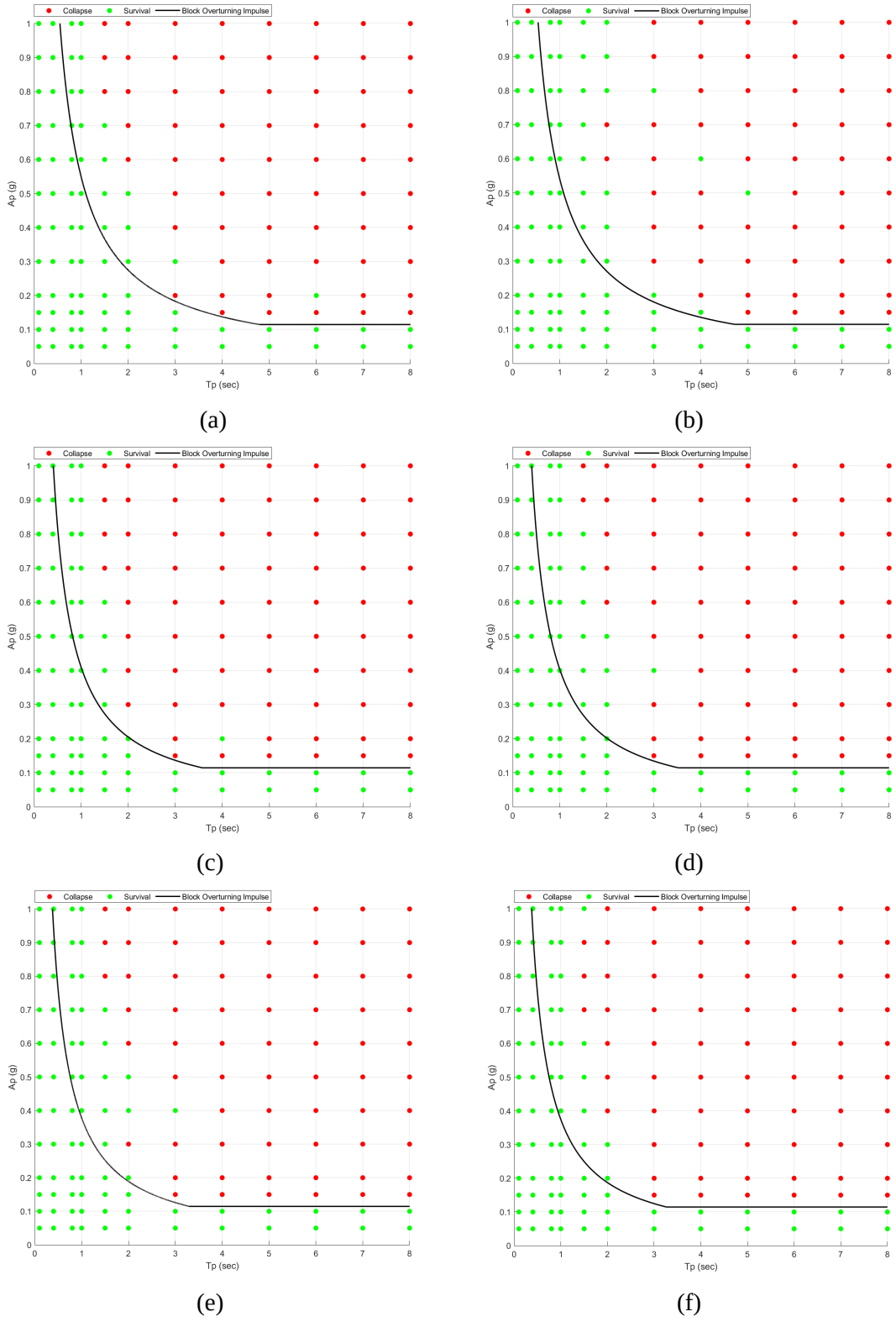

Figure 8: Charts showing stability of Iaat column under idealized near-fault ground excitation (friction angle of 26°) (a) γ=1 and ν=0 (b) γ=1 and ν=90 (c) γ=2 and ν=0 (d) γ=2 and ν=90 (e) γ=3 and ν=0 (f) γ=3 and ν=90.

The near-fault ground excitations that represent real earthquake records were applied to the column to analyze their dynamic response. The near-fault pulses were obtained from the realistic synthetic ground motions produced by Mavroeidis & Apostolos (2003). The synthetic ground motions are adequate for engineering analysis and design. Figure 9 shows the results of the numerical simulations of Baalbek and Iaat column under 40 near-fault ground excitations that represent recorded earthquakes. The green dot shows that the column has survived the applied seismic excitation. The red dot shows that the column has overturned under the applied seismic excitation. The mode of collapse of Baalbek and Iaat column for the earthquake pulses is shown in Tables 8 and 9, respectively.

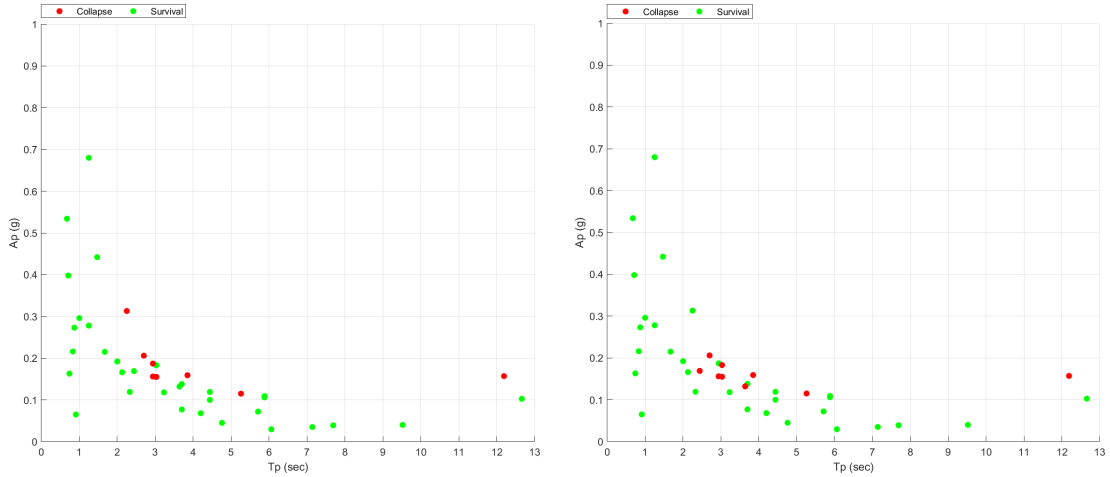

(a) (b)

Figure 9: Charts showing stability of the column under earthquake pulses (friction angle of 26°) (a) Baalbek column (b) Iaat column.

Table 8: Mode of collapse of Baalbek column for earthquake pulses.

	Pulse 5a	Pulse 7c	Pulse 7e	Pulse 12a	Pulse 17c	Pulse 17d	Pulse 17e	Pulse 20b
Side View								
Top View								

Table 9: Mode of collapse of Iaat column for earthquake pulses.

	Pulse 5a	Pulse 7c	Pulse 7d	Pulse 7e	Pulse 15a	Pulse 17a	Pulse 17d	Pulse 17e	Pulse 20b
Side View									
Top View									

4.2 Effect of changing the values of γ and ν on the mode of collapse of the columns

The mode of collapse of Baalbek and Iaat column under the six near-fault ground excitations were plotted in Tables 10 and 11, respectively. Different markers were used to indicate the mode of collapse (Total or partial) and the direction of movement (in-plane or out-of-plane).

Mode of collapse of Baalbek column for different near-fault ground excitations:

- At large periods, total collapse of the column was observed for all the near-fault ground excitations.
- At intermediate periods, wobbling and partial collapse was observed the most for near-fault ground excitations with ν = 90°.
- At small periods, less than 1s, the column survived all the near-fault ground excitations.
- The stability of the column is affected by the value of γ. As γ increases, the number of oscillations in the pulse increases. As shown in table 10, for γ=1 and Tp=1.5s, no collapse was observed. However, collapse was observed for γ=2 and γ=3 at Tp=1.5s.

Mode of collapse of Baalbek column for different near-fault ground excitations:

- Total collapse of the column was observed at large periods for all near-fault ground excitations.
- Partial collapse was observed at intermediate periods at high acceleration values for ν = 0° and at lower acceleration values for ν = 90°.
- As γ increases, the column collapse at lower acceleration values due to the increase in the number of oscillations as shown in table 11.

Table 10: Mode of collapse of Baalbek column as function of γ and ν (friction angle of 26°).

ν / γ	0	90
1	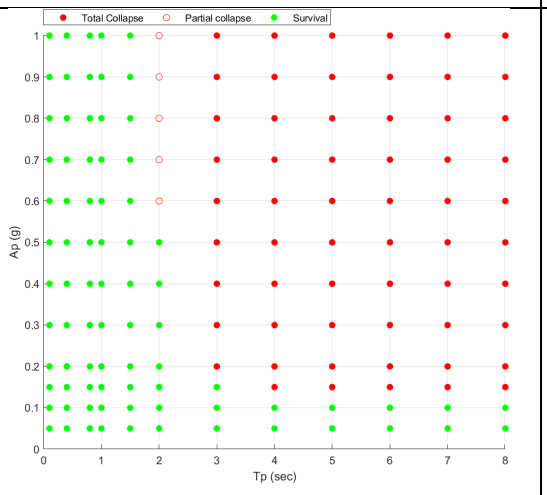	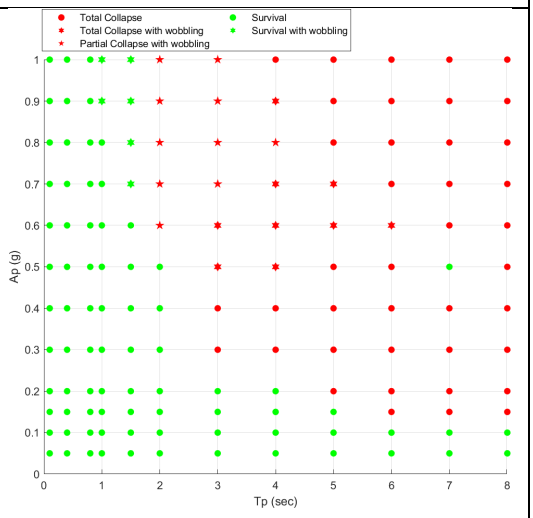
2	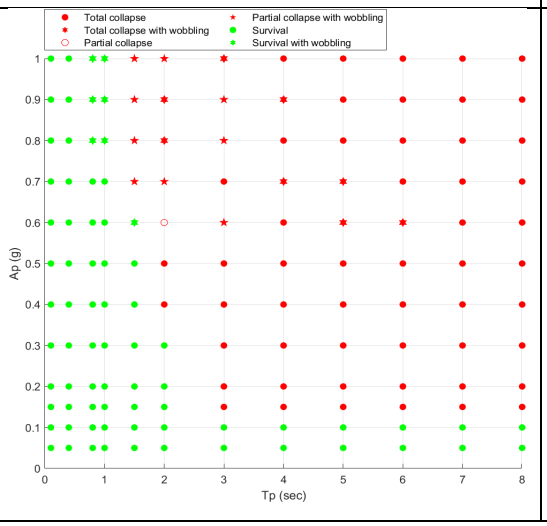	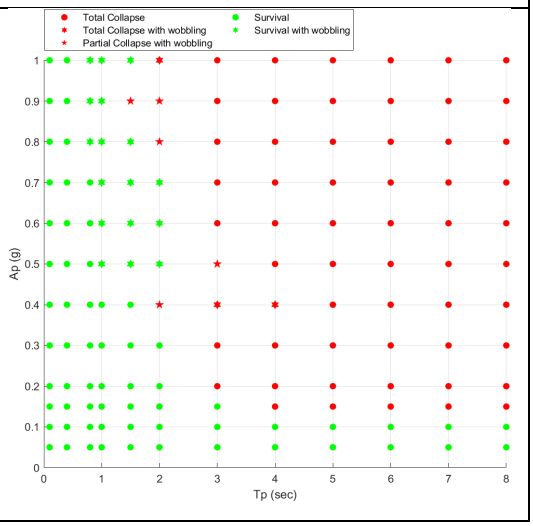

3	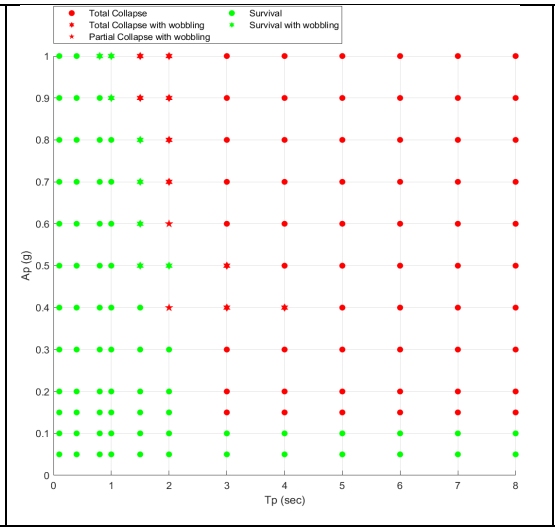	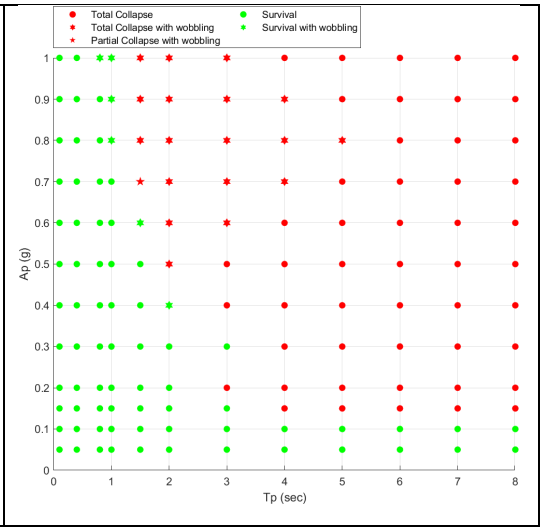

Table 11: Mode of collapse of Iaat column as function of γ and ν (friction angle of 26°).

ν / γ	0	90
1	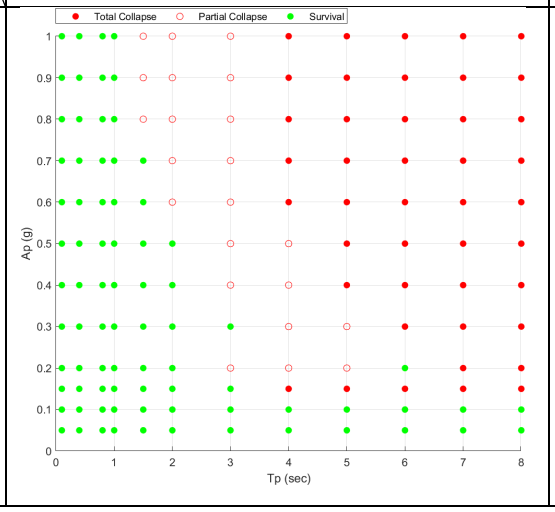	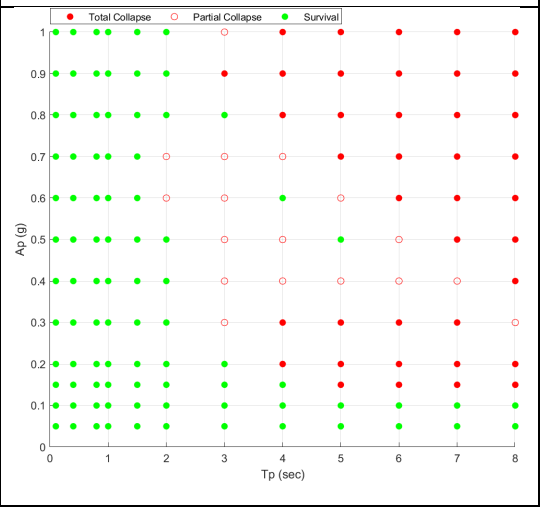

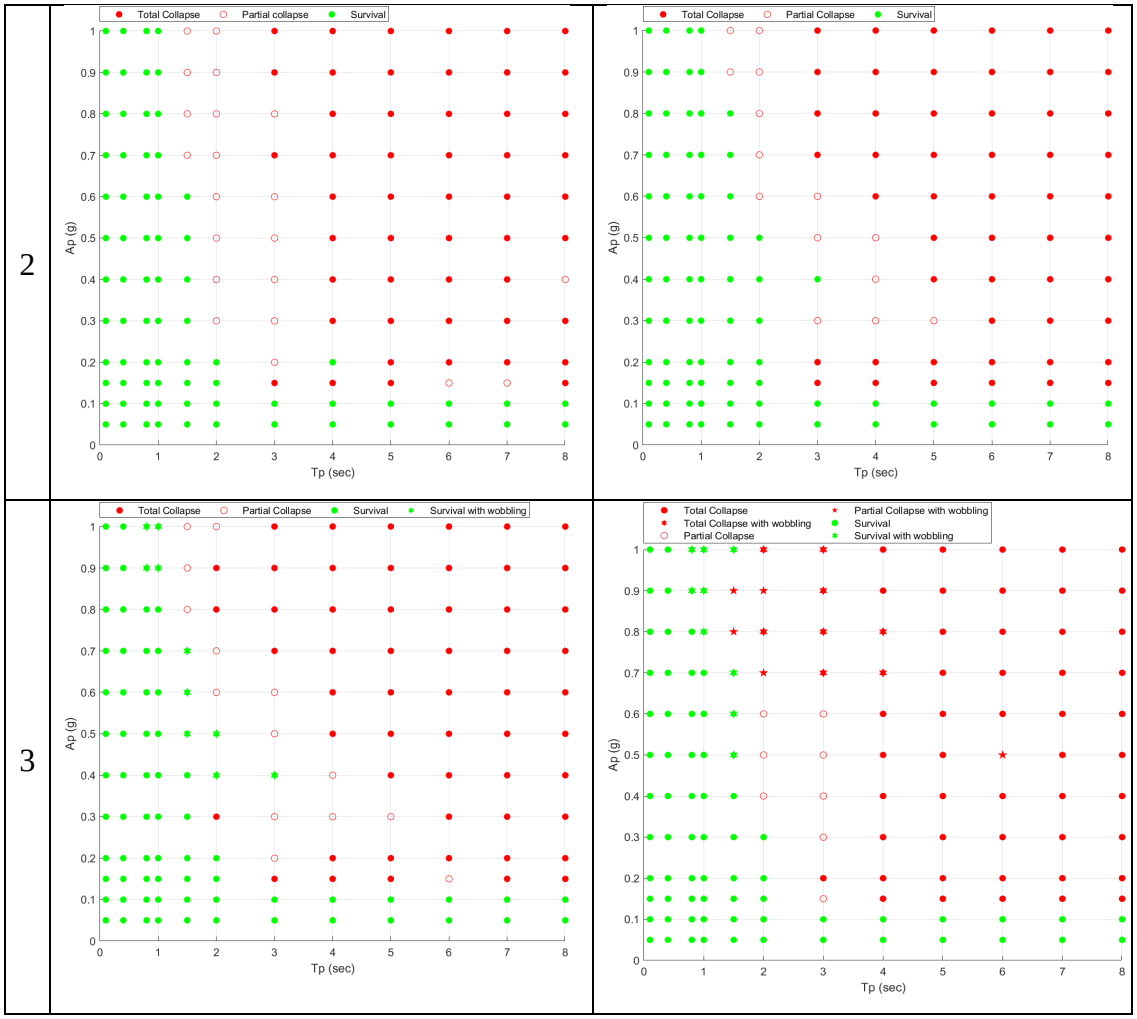

4.3 Dynamic response of Baalbek and Iaat columns using theoretical modeling

The theoretical modeling results are illustrated in the charts as a black curve representing the critical block overturning impulse plotted using the analytical model developed by Tabbara & Karam (2019) (Figures 7 and 8). The critical block overturning impulse curve was plotted for each column. The 3DEC boundaries and safe-unsafe boundary of the simplified theoretical modelling agree well. At periods lower than the transition point Tp, the required accelerations for overturning grow hyperbolically as per Equation 2. At periods larger than the transition point Tp, the numerical and theoretical modeling are in perfect agreement where the rocking limit αg dominates as per equation 1. The columns

survived for all pulses with acceleration lower than αg for both numerical and theoretical modeling. The calculated transition points observed are not far from those calculated by equation 3. At intermediate periods, there was a slight difference in the safe-unsafe boundaries for theoretical and numerical modeling. The differences in the results of each approach reflect differences in the level of precision and the number of parameters included in each approach. The theoretical modeling was developed for a single block, while the numerical modeling was performed for multi-drum columns.

4.4 Estimates of the ground motion parameters of historical earthquakes

The purpose of the study is to estimate the ground motion parameters of historical earthquakes that hit in the Bekaa valley. The previous earthquakes caused the columns of Baalbek from Temple of Jupiter to collapse, however the free-standing column in Iaat survived. Figure 10 shows all the near-fault ground excitations applied to the columns as grey dots, a plus marker is plotted for a specific pulse if it caused the collapse of Baalbek column and the survival of the Iaat column. A total of eight pulses with different periods and accelerations were obtained. To be more precise, the response of the column to each pulse was observed in order to identify the pulses that caused offset of the capital of Iaat column (as its current position). The response of Baalbek and Iaat columns at the end of each pulse is shown in Table 12. The pulses that do not fit the shape of the column today with the offset at the top were eliminated. A cross marker was plotted for the pulses that caused the offset at the capital of Iaat column. The star marker shows the combinations of period and acceleration of the four critical pulses obtained. Iaat column survived for all the critical pulses with a displacement at the column's capital and Baalbek column collapsed for all the critical pulses. Moreover, two of the synthetic pulses that represents real earthquakes, caused the collapse of Baalbek column and the survival of Iaat column with offset of the capital. However, the offset at the top of Iaat column due to the near-fault ground motions that replicates Superstition Hills earthquake and Northridge earthquake is very small.

The critical pulses' acceleration, velocity, and displacement time histories are plotted in Figure 11. The pulses have intermediate and large periods, with acceleration ranging from 0.4g to 1.0g. As the period of the pulse increases, the critical acceleration of the pulse becomes smaller. All the pulses have a value of nu equal to 90°, four pulses have a value of gamma equal to 1, and one pulse has a value of gamma equal to 12.

Fayjaloun et al. (2021) proposed a hybrid simulation of near-fault ground motion for an earthquake along the Yammouneh fault with a magnitude of 7. The results indicate that the median peak ground acceleration for sites located at 5 km from the Yammouneh fault ranges from 0.31g to 0.46g. The sites that are 25 km away from the Yammouneh fault have peak ground acceleration between 0.13g and 0.19g. The results in this study show that the obtained near-fault ground motions on the historical earthquakes have a minimum peak ground acceleration of 0.4g. This value confirms with the values obtained by Fayjaloun et al. (2021) for the sites located near the Yammouneh fault (at 5 km). However, the peak ground acceleration range for the sites located at 25 km from the fault may be underestimated. This is because the temple of Baalbek is located approximately 20 km away from the Yammouneh fault, and the 1202 earthquake that occurred along the Yammouneh fault caused the collapse of 31 columns of the Temple of Jupiter (Ambraseys & Barazangi, 1989). Therefore, higher acceleration values than 0.13g to 0.19g are required to cause collapse to the columns of Baalbek (Baalbek column survived under all pulses with acceleration lower than 0.15g).

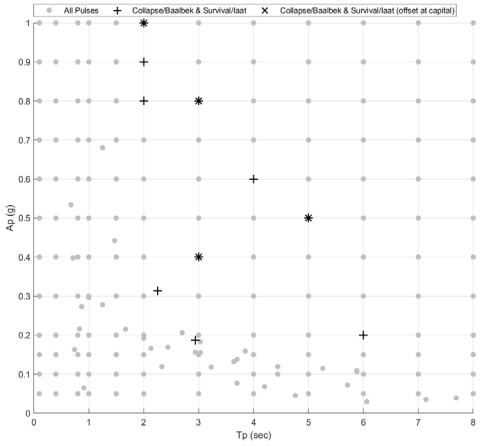

Figure 10: Chart showing the combination of periods and accelerations of near-fault ground excitation that led to the collapse of Baalbek and survival of Iaat (friction angle of 26°).

Table 12: Survival of Iaat column and collapse of Baalbek column under specific pulses (friction angle of 26°).

Tp=2s & Ap=1.0g (γ=1 &ν=90°)	Tp=2s & Ap=0.9g (γ=1 &ν=90°)	Tp=2s & Ap=0.8g (γ=1 &ν=90°)	Tp=3s & Ap=0.8g (γ=1 &ν=90°)
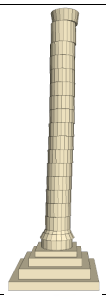	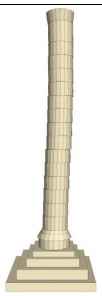	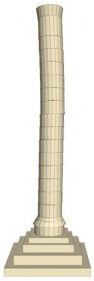	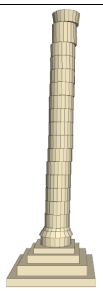
	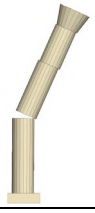	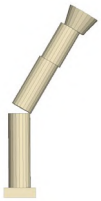	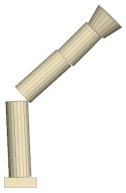

Tp=3s & Ap=0.4g (γ=2 &ν=90°)	Tp=4s & Ap=0.6g (γ=1 &ν=90°)	Tp=5s & Ap=0.5g (γ=1 &ν=90°)	Tp=6s & Ap=0.2g (γ=1 &ν=0°)
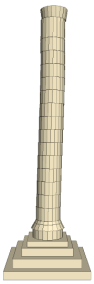	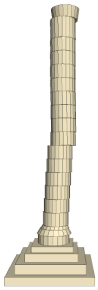	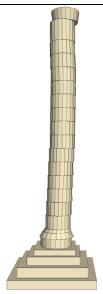	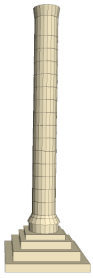
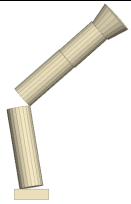	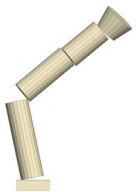	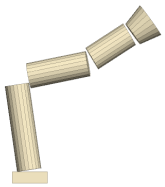	

Tp=2.25 & Ap=0.313g (12a)	Tp=2.94 & Ap=0.187g (17c)
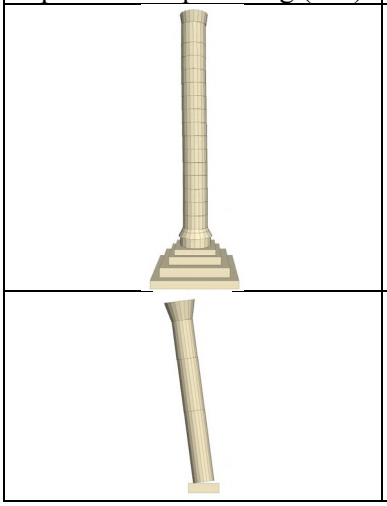	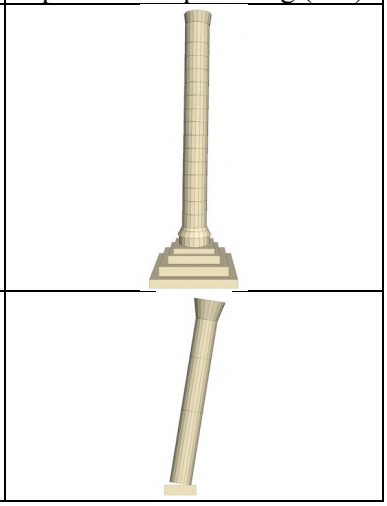

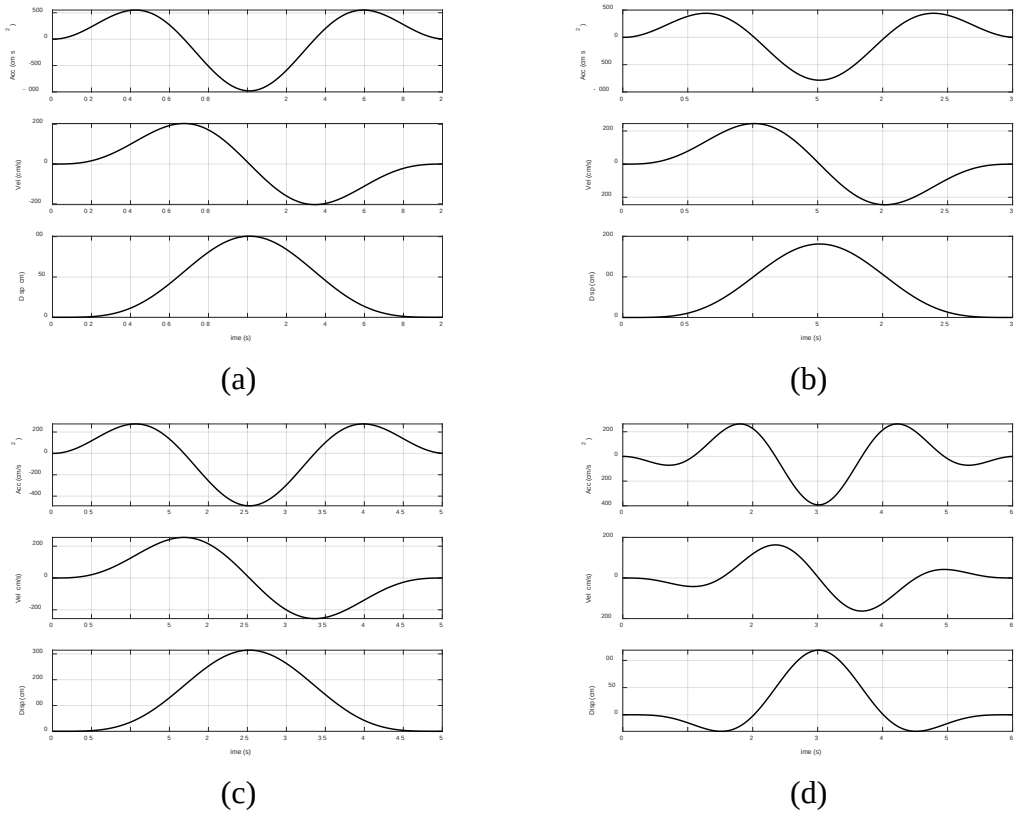

(a) (b)

(c) (d)

Figure 11: Acceleration, velocity, and displacement time histories of the critical pulses (a) Ap=1.0g and Tp=2s (γ=1 and ν=90°) (b) Ap=0.8g and Tp=3s (γ=1 and ν=90°) (c) Ap=0.5g and Tp=5s (γ=1 and ν=90°) (d) Ap=0.4g and Tp=3s (γ=2 and ν=90°).

4.5 Friction analysis

The friction coefficient used in the numerical simulations of Baalbek and Iaat columns was obtained by the experimental program carried out on reduced scale columns of Baalbek (0.5 and 1m columns) (Tabbara & Karam (2019)). The friction coefficient measured from the shaking tables, μ=0.448 (26°), falls within the range of values determined experimentally going from μ=0.25 to μ=0.75 (Drosos & Anastasopoulos, 2014; Pitilakis et al., 2017; Sarhosis et al., 2016). However, some researchers adopted higher friction factors to consider the effect of the reduced scaled columns and to better reproduce full scale structures (Psycharis et al., 2000; Psycharis & Ambraseys, 2011). A sensitivity analysis on the effect of friction coefficient on the response of the full-scale multi-drum columns was performed for μ=0.75 (37°).

The mode of collapse of Baalbek and Iaat column under near-fault ground excitation with γ=1 and ν=0 is shown in Tables 13 and 14, respectively. The columns show similar mode of collapse for both friction coefficients. At large periods, total collapse is observed for both columns. At intermediate periods, partial collapse was observed. The columns survived all the acceleration values at small periods.

The numerical modelling results were plotted in charts to determine the stability of the column under the 6 types of idealized near-fault ground excitations for friction angle equal to 37° (Figures 12 and 13). The results shows that the stability of Baalbek column is not affected by the friction coefficient, whereas the change in the friction coefficient affects the stability of Iaat column. Iaat column survived for near-fault ground excitations (γ=1 and ν=90°) at T_p=2s and A_p=0.8g and 0.9g, T_p=4s and A_p=0.6g, and T_p=5s and A_p=0.5g for friction angle of 26° and collapsed for friction angle of 37° under the same pulses. This was also observed for near-fault ground excitations (γ=3 and ν=0°) at T_p=3s and A_p=0.4g and for near-fault ground excitations (γ=3 and ν=90°) at T_p=1.5s and A_p=0.7g.

The dynamic response of Baalbek and Iaat column under pulses that represent recorded near-fault ground excitation (earthquakes) is the same for both friction angles (26° and 37°). The mode of failure of Baalbek and Iaat column under earthquake pulses with

friction angle equal to 37° were plotted in Figure 14, the same results were observed for friction angle equal to 26°.

Figure 15 shows the combined charts for all near-fault ground excitations, the pulses that caused collapse to Baalbek column and survival to Iaat column were shown in black plus markers. The results shows that only four pulses satisfy this condition for friction angle equal to 37°, whereas eight pulses were obtained for friction angle equal to 26°. The dynamic response of the columns was observed to choose the pulses that caused collapse of Baalbek column and survival of Iaat column with offset at the top (Table 15). The pulses that caused offset at the capital of Iaat column were shown as black cross markers. Three pulses were obtained with acceleration ranging from 0.4g to 1.0g and periods equal to 2 and 3s.

Table 13: Mode of collapse of Baalbek column under near-fault ground excitations (γ=1 and ν=0) with different combinations of periods and accelerations (friction angle of 37°) (a) Side view (b) Top view.

Ap \ Tp	0.1	0.4	0.8	1	1.5	2	3	4	5	6	7	8
1.0g	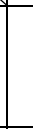				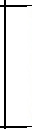	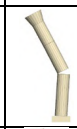		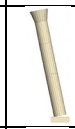	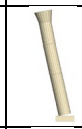	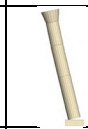		
0.9g	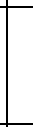			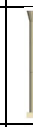		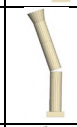		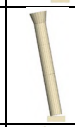	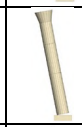	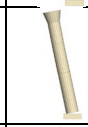		
0.8g	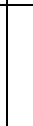					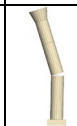		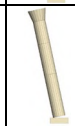	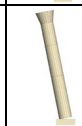	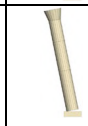		
0.7g	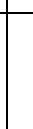											
0.6g												
0.5g												
0.4g												

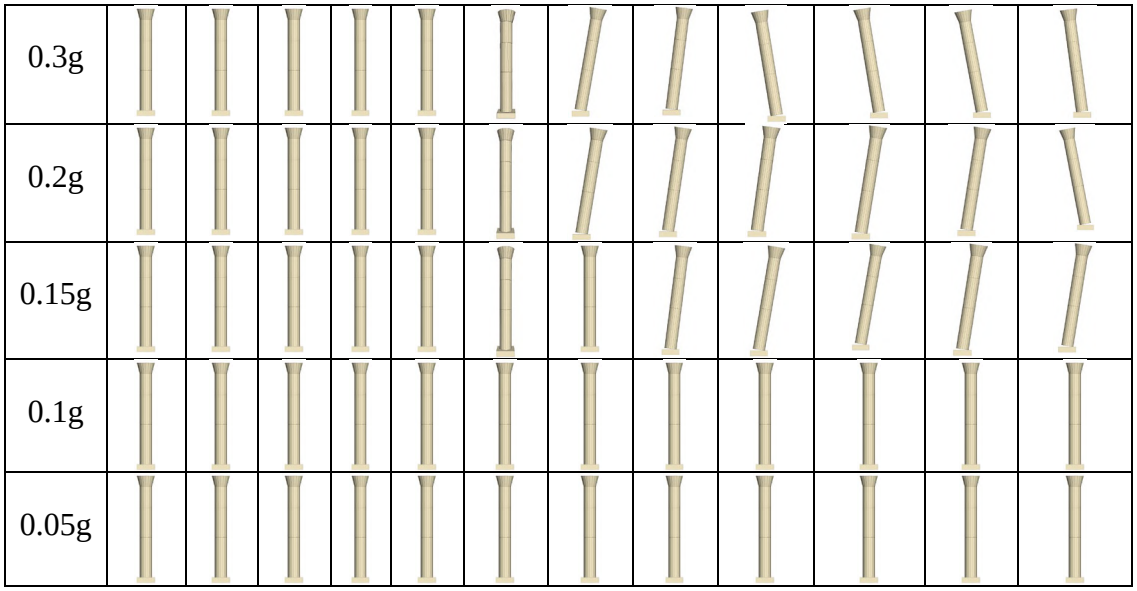

(a)

Tp / Ap	0.1	0.4	0.8	1	1.5	2	3	4	5	6	7	8
1.0g	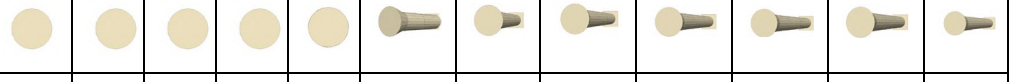											
0.9g	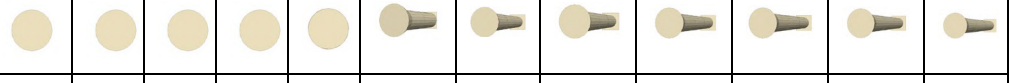											
0.8g	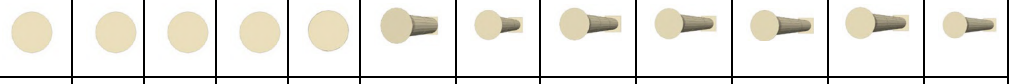											
0.7g	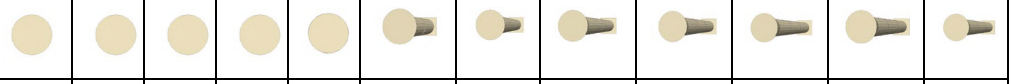											
0.6g												
0.5g	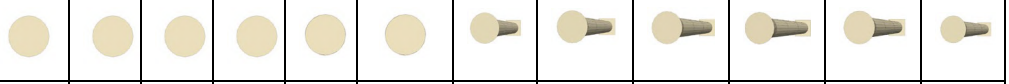											
0.4g	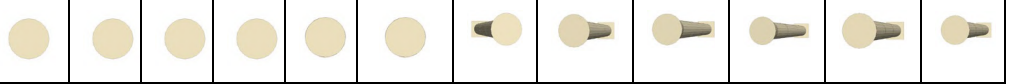											
0.3g	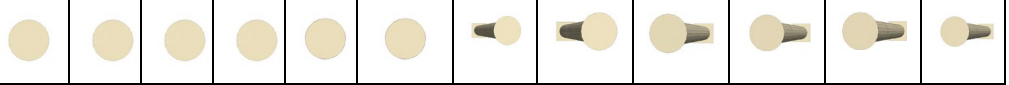											
0.2g												
0.15g	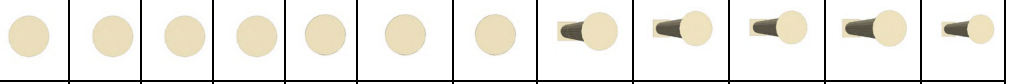											
0.1g	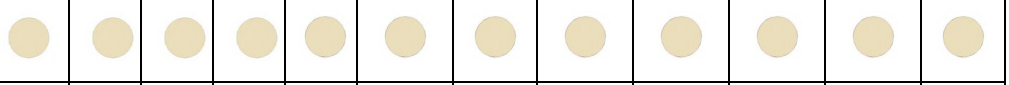											
0.05g	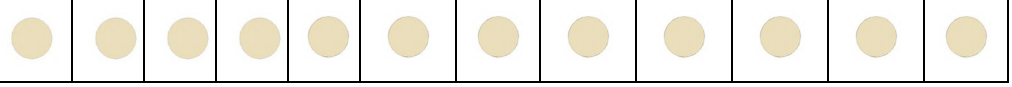											

(b)

Table 14: Mode of collapse of Iaat column under near-fault ground excitations (γ=1 and ν=0) with different combinations of periods and accelerations (friction angle of 37°) (a) Side view (b) Top view.

Ap \ Tp	0.1	0.4	0.8	1	1.5	2	3	4	5	6	7	8
1.0g	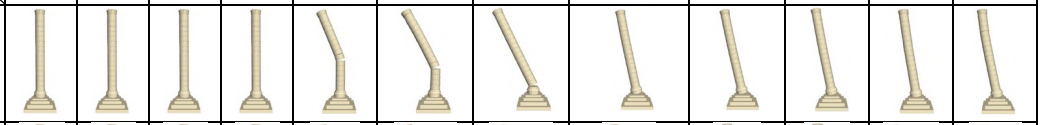											
0.9g	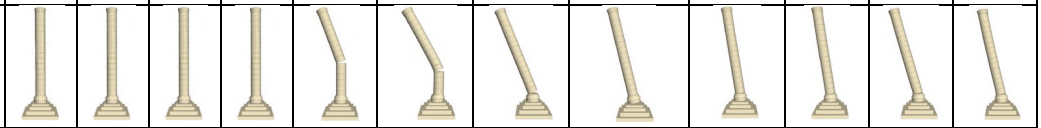											
0.8g	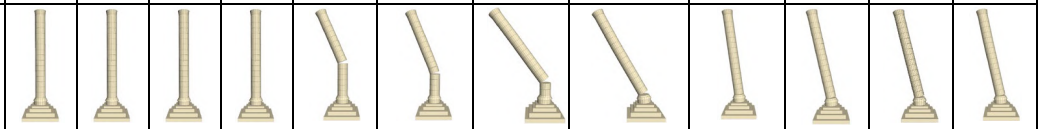											
0.7g	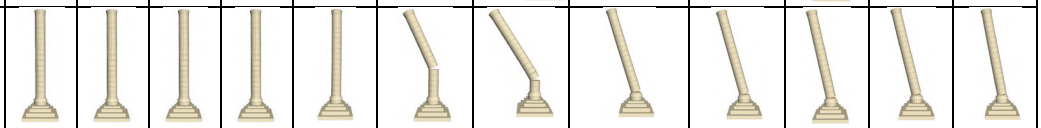											
0.6g												
0.5g												
0.4g	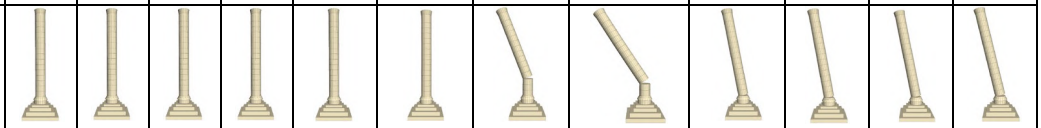											
0.3g	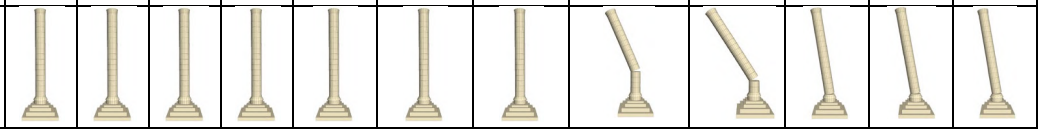											
0.2g	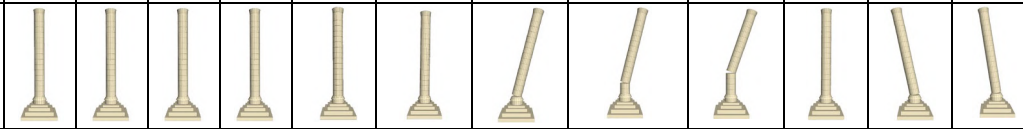											
0.15g	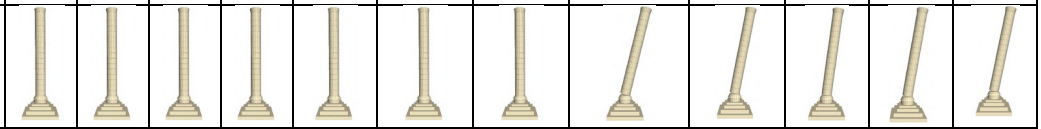											
0.1g	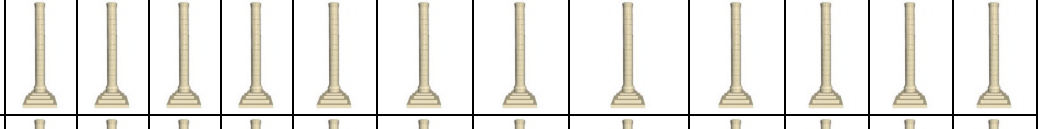											
0.05g	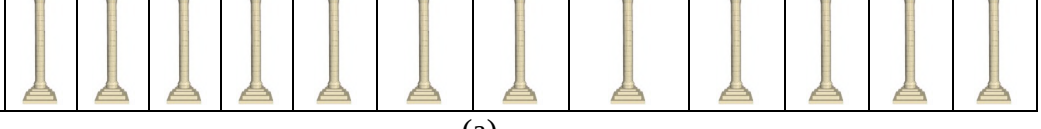											

(a)

Tp / Ap	0.1	0.4	0.8	1	1.5	2	3	4	5	6	7	8
1.0g												
0.9g												
0.8g												
0.7g												
0.6g												
0.5g												
0.4g												
0.3g												
0.2g												
0.15g												
0.1g												
0.05g												

(b)

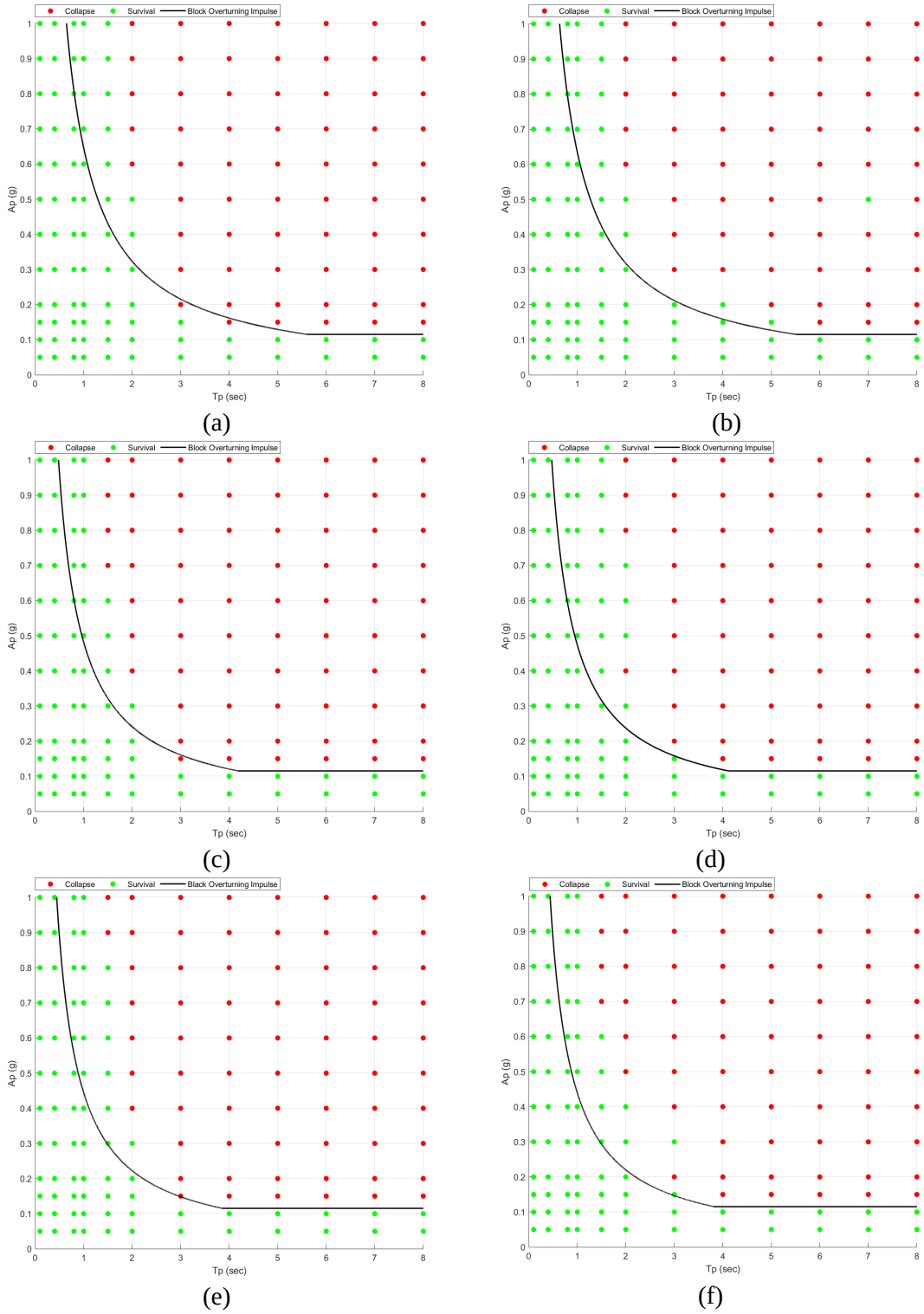

Figure 12: Charts showing stability of Baalbek column under near-fault ground excitation (friction angle of 37°) (a) γ=1 and ν=0 (b) γ=1 and ν=90 (c) γ=2 and ν=0 (d) γ=2 and ν=90 (e) γ=3 and ν=0 (f) γ=3 and ν=90.

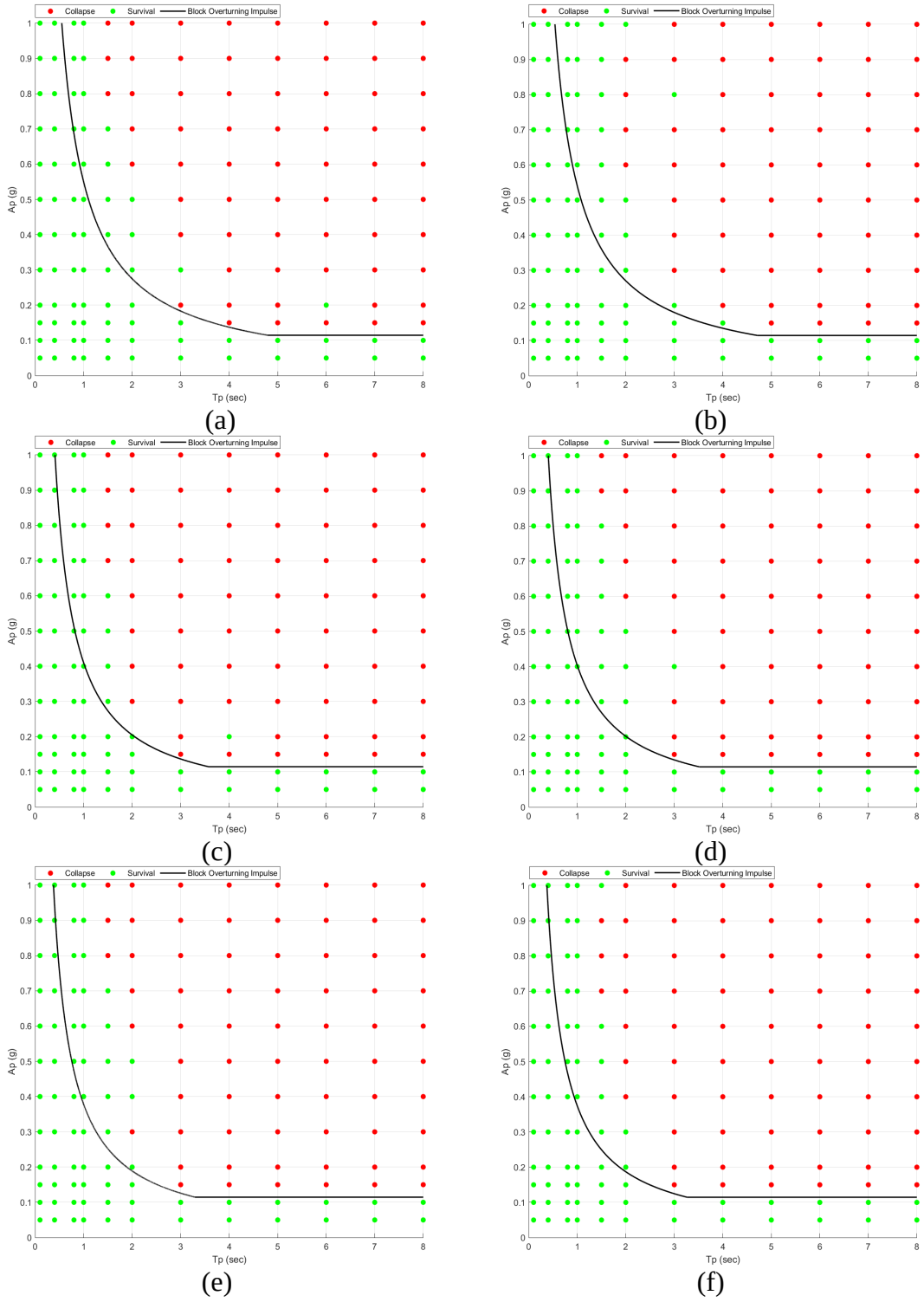

Figure 13: Charts showing stability of Iaat column under near-fault ground excitation (friction angle of 37°) (a) γ=1 and ν=0 (b) γ=1 and ν=90 (c) γ=2 and ν=0 (d) γ=2 and ν=90 (e) γ=3 and ν=0 (f) γ=3 and ν=90.

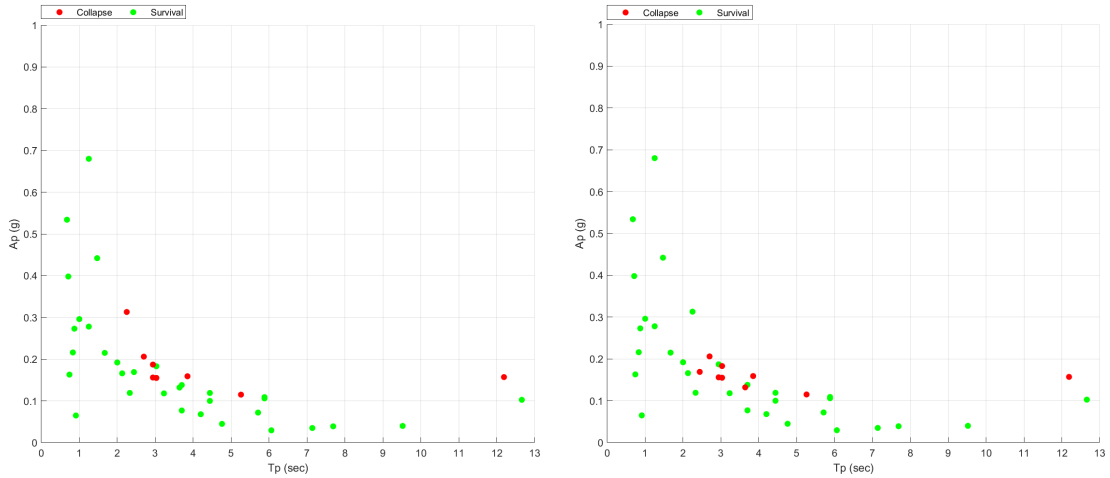

(a) (b)

Figure 14: Charts showing stability of the column under earthquake pulses (friction angle of 37°) (a) Baalbek column (b) Iaat column.

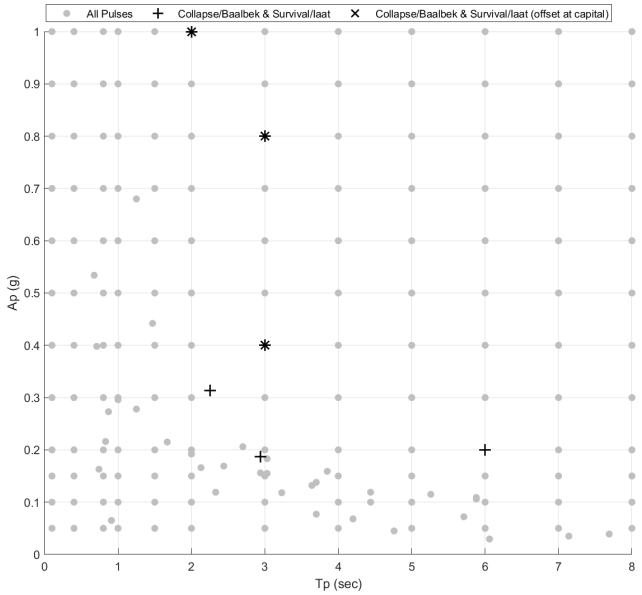

Figure 15: Chart showing the combination of periods and accelerations of near-fault ground excitation that led to the collapse of Baalbek and survival of Iaat (friction angle of 37°).

Table 15: Survival of Iaat column and collapse of Baalbek column under critical pulses (friction angle of 37°).

Tp=2s & Ap=1.0g (γ=1 &ν=90°)	Tp=3s & Ap=0.8g (γ=1 &ν=90°)	Tp=3s & Ap=0.4g (γ=2 &ν=90°)	Tp=6s & Ap=0.2g (γ=1 &ν=0°)
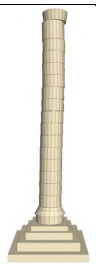	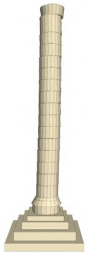	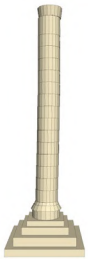	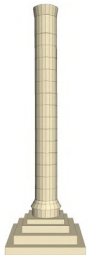
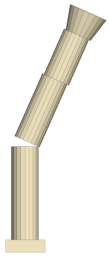	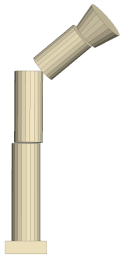	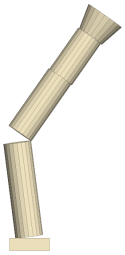	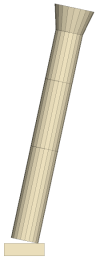

Tp=2.25 & Ap=0.313g (12a)	Tp=2.94 & Ap=0.187g (17c)
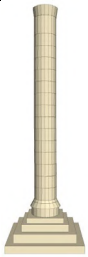	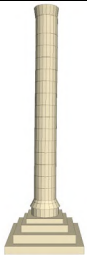
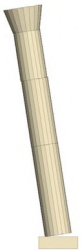	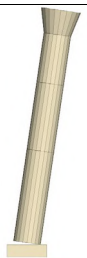

4.6 Magnitude and Intensity of historical earthquakes in Lebanon

Previous studies on the historical earthquakes in Lebanon revealed the Magnitude and Intensity of the seismic activities. Therefore, the pulses were shown in terms of magnitude and intensity to validate our results. Figures 16 shows the magnitude and intensity of the pulses for friction angle equal to 26° as a plus sign and for friction angle equal to 37° as a cross sign, respectively. Therefore, overlap between the pulses shows as a star. Mavroeidis & Apostoloss (2003) developed an empirical relationship between the period of the near-fault ground excitations and the moment magnitude (Mw). By comparing the intensities of eight significant earthquakes in California to the horizontal peak ground motions, Wald et al., (1999) developed regression relationships between peak ground acceleration and Modified Mercalli Intensity. According to equations (5) and (6), the pulse period was converted to magnitude and the horizontal acceleration was converted to intensity.

$$\log Tp = -2.9 + 0.5\,Mw \qquad (8)$$

$$I = 3.66 \log(PGA) - 1.66 \qquad (9)$$

The results shows that the previous earthquakes have Intensity of VIII or IX and magnitude that ranges from 6.4 to 7.2. These findings are consistent with previous research on the magnitude and intensity of historical earthquakes. According to Ambraseys & Melville (1988), the 1202 earthquake has an intensity value IX in the Bekaa valley and magnitude equals to 7.6 (Figure 17a). Moreover, Ambraseys & Barazangi (1989) showed that the 1759 earthquake has an intensity value VIII in the Bekaa valley and magnitude equals to 6.6 for the first shock in October and 7.4 for the second shock in November (Figure 17b).

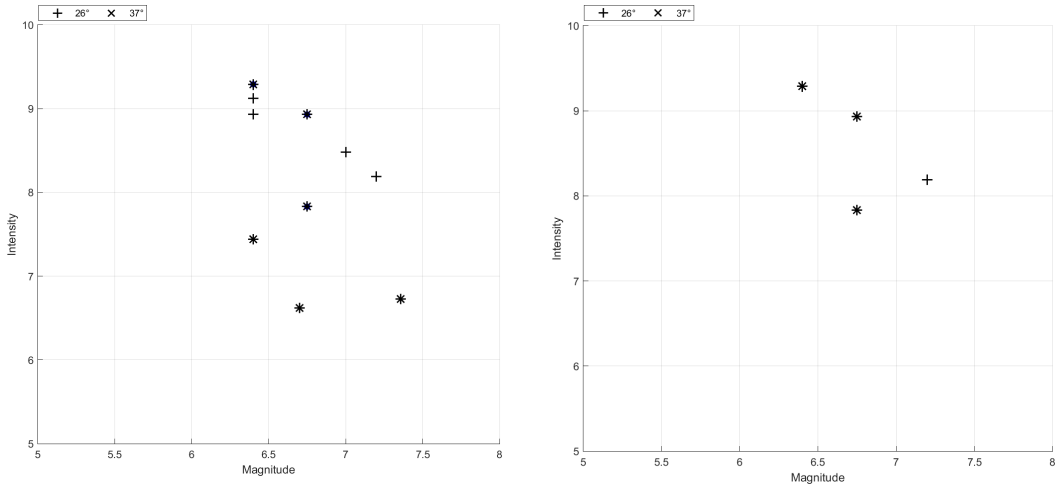

Figure 16: Chart showing the combination of magnitude and intensity of near-fault ground excitation for both friction angles (26° and 37°) that led to (a) the collapse of Baalbek and survival of Iaat (b) the collapse of Baalbek and survival of Iaat with offset of the capital.

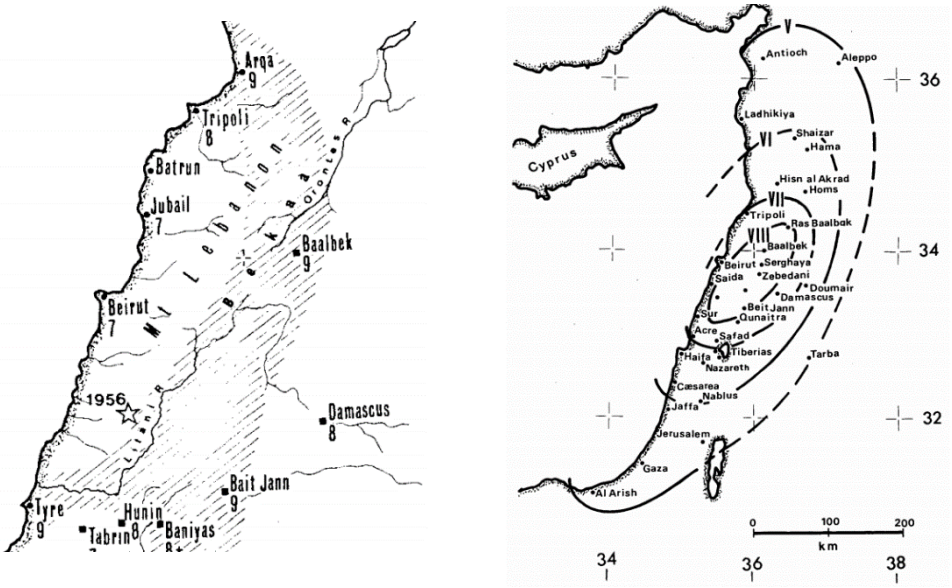

Figure 17: Intensity distribution in MSK scale of (a) the 1202 earthquake (b) the 1759 earthquake (Ambraseys & Melville, 1988; Ambraseys & Barazangi, 1989).

Chapter Five

Conclusion

Studying the dynamic response of ancient columns that have been exposed to historical earthquakes is an important task that serves in estimating the ground motion parameters of ancient earthquakes based on archaeological evidence. This study investigated the seismic response of Baalbek and Iaat columns when subjected to near-fault ground excitations with varying periods and accelerations. The dynamic response of the columns was investigated using numerical modeling based on the distinct element method. The numerical modeling results were compared to a simple theoretical block overturning impulse. Based on the obtained results, the following conclusions can be drawn:

Estimates on the ground motion parameters of historical earthquakes:

- The near-fault ground excitations of the historical earthquakes have intermediate and large periods (Tp = 2,3, and 5s) with acceleration values ranging from 0.4g to 1.0g.
- The numerical modeling results show that the historical earthquakes had Intensities of VIII or IX and Magnitudes ranging from 6.4 to 7.2.
- These values agree well with previous investigations on historical earthquakes in Lebanon: The 1202 earthquake has intensity of IX near Baalbek and a magnitude Mw = 7.6 and the 1759 earthquake has intensity of VIII near Baalbek a magnitude Mw=7.4.

Dynamic response of multi-drum columns:

- The 3DEC results of Baalbek column subjected to near-fault ground excitations are in good agreement with the 3DEC results of Baalbek column under 25 cycles of cosine pulse. At high periods, the multi-drum column behaves monolithically, and total collapse is observed. At intermediate periods, rocking and wobbling is observed that leads to out of plane collapse of the column. At small periods,

wobbling at the top of the column is observed. A shift in the transition period is observed.

- Higher accelerations are required to cause collapse to Baalbek column under a near-fault ground excitation than those required for 25 cycles of a cosine pulse.
- The safe-unsafe boundaries of Baalbek and Iaat column under near-fault ground excitations are similar.
- The difference in the number of drum of each column affects the mode of collapse. Wobbling was observed more for Baalbek column. Partial collapse was observed more for Iaat column.
- The friction coefficient has no effect on the stability of Baalbek column and a small effect on the stability of Iaat column. Survival of Iaat column was observed for friction angle equal to 26° while the column collapsed for friction angle equal to 37° under the same pulses.
- The block overturning impulse can be used as a good estimate to identify the stability of the columns.

References

Ambraseys, N. N., & Barazangi, M. (1989). The 1759 earthquake in the bekaa valley: Implications for earthquake hazard assessment in the eastern mediterranean region. *Journal of Geophysical Research: Solid Earth, 94*(B4), 4007-4013. doi:10.1029/JB094iB04p04007

Ambraseys, N. N., & C. P. Melville. (1988). An analysis of the eastern mediterranean earthquake of 20 may 1202. *History of Seismography and Earthquakes of the World, ,* 181-200.

Ambraseys, N. N., & Jackson, J. A. (1998). Faulting associated with historical and recent earthquakes in the eastern mediterranean region. *Geophysical Journal International, 133*(2), 390-406. doi:10.1046/j.1365-246X.1998.00508.x

Ben-Menahem, A. (1991). Four thousand years of seismicity along the dead sea rift. *Journal of Geophysical Research: Solid Earth, 96*(B12), 20195-20216. doi:10.1029/91JB01936

Cundall, P. A. (1971). A computer model for simulating progressive large scale movements in blocky rock systems. *Proceedings of the Symposium of the International Society for Rock Mechanics, Society for Rock Mechanics (ISRM), France.,* (II-8)

Daëron, M., Klinger, Y., Tapponnier, P., Elias, A., Jacques, E., & Sursock, A. (2007). 12,000-year-long record of 10 to 13 paleoearthquakes on the yammoûneh fault, levant fault system, lebanon. *Bulletin of the Seismological Society of America, 97*(3), 749-771. doi:10.1785/0120060106

Dimitri, R., De Lorenzis, L., & Zavarise, G. (2011). Numerical study on the dynamic behavior of masonry columns and arches on buttresses with the discrete element method. *Engineering Structures, 33*(12), 3172-3188. doi:10.1016/j.engstruct.2011.08.018

Drosos, V. A., & Anastasopoulos, I. (2015). Experimental investigation of the seismic response of classical temple columns. *Bulletin of Earthquake Engineering, 13*(1), 299-310. doi:10.1007/s10518-014-9608-y

Drosos, V., & Anastasopoulos, I. (2014). Shaking table testing of multidrum columns and portals. *Earthquake Engineering & Structural Dynamics, 43*(11), 1703-1723. doi:10.1002/eqe.2418

Ellenblum, R., Marco, S., Agnon, A., Rockwell, T., & Boas, A. (1998). Crusader castle torn apart by earthquake at dawn, 20 may 1202. *Geology (Boulder), 26*(4), 303-306. doi:10.1130/0091-7613(1998)0262.3.CO;2

Fayjaloun, R., Dabaghi, M., Cornou, C., Causse, M., Lu, Y., Stehly, L., . . . Mariscal, A. (2021). Hybrid simulation of Near-Fault ground motion for a potential mw 7 earthquake in lebanon. *Bulletin of the Seismological Society of America, 111*(5), 2441-2462. doi:10.1785/0120210091

Foti, D., & Vacca, V. (2017). *Experimental investigation of the seismic response of a multi-drum column*. Southampton, United Kingdom Southampton, Southampton: W I T Press. doi:http://dx.doi.org/10.2495/CMEM170021

FOTI, D., & VACCA, V. (2017). Rocking of multiblock stone classical columns. *WIT Transactions on the Built Environment, 172*, 1. doi:10.2495/ERES170011

Galadini, F., Hinzen, K., & Stiros, S. (2006). Archaeoseismology: Methodological issues and procedure. *Journal of Seismology, 10*(4), 395-414. doi:10.1007/s10950-006-9027-x

Gomez, F., Meghraoui, M., Darkal, A. N., Sbeinati, R., Darawcheh, R., Tabet, C., . . . Barazangi, M. (2001). Coseismic displacements along the serghaya fault; an active branch of the dead sea fault system in syria and lebanon. *Journal of the Geological Society, 158*(3), 405-408. doi:10.1144/jgs.158.3.405

Gomez, F., Meghraoui, M., Darkal, A. N., Hijazi, F., Mouty, M., Suleiman, Y., . . . Barazangi, M. (2003). Holocene faulting and earthquake recurrence along the serghaya branch of the dead sea fault system in syria and lebanon. *Geophysical Journal International, 153*(3), 658-674. doi:10.1046/j.1365-246X.2003.01933.x

Grigoratos, I., Poggi, V., Danciu, L., & Rojo, G. (2020). An updated parametric catalog of historical earthquakes around the dead sea transform fault zone. *Journal of Seismology, 24*(4), 803-832. doi:10.1007/s10950-020-09904-9

Hinzen, K. (2009). Simulation of toppling columns in archaeoseismology. *Bulletin of the Seismological Society of America, 99*(5), 2855-2875. doi:10.1785/0120080241

Housner, G. W. (1963). The behavior of inverted pendulum structures during earthquakes. *Bulletin of the Seismological Society of America, ,* 403-417.

Huijer, C., Harajli, M., & Sadek, S. (2016). Re-evaluation and updating of the seismic hazard of lebanon. *Journal of Seismology, 20*(1), 233-250. doi:10.1007/s10950-015-9522-z

Itasca Consulting Group Inc. (2019). 3DEC - 3 dimensional distinct element code, version 5.2 [computer software]. User's Guide. Minneapolis, USA:

Karam, G., & Tabbara, M. (2020). Rocking blocks stability under critical pulses from near-fault earthquakes using a novel energy based approach. *Applied Sciences, 10*(17), 5924. doi:10.3390/app10175924

Karavasilis, T. L., Makris, N., Bazeos, N., & Beskos, D. E. (2010). Dimensional response analysis of multistory regular steel MRF subjected to pulselike earthquake ground motions. *Journal of Structural Engineering, 136*(8), 921-932. doi:10.1061/(ASCE)ST.1943-541X.0000193

Khair, K., Karakaisis, G. F., & Papadimitriou, E. E. (2000). Seismic zonation of the dead sea transform fault area. *Annali Di Geofisica, 43*(1), 61-79. doi:10.4401/ag-3620

Koh, A., & Mustafa, G. (1990). Free rocking of cylindrical structures. *Journal of Engineering Mechanics, 116*(1), 35-54. doi:10.1061/(ASCE)0733-9399(1990)116:1(35)

Komodromos, P., Papaloizou, L., & Polycarpou, P. (2008). Simulation of the response of ancient columns under harmonic and earthquake excitations. *Engineering Structures, 30*(8), 2154-2164. doi:10.1016/j.engstruct.2007.11.004

Konstantinidis, D., & Makris, N. (2005). Seismic response analysis of multidrum classical columns. *Earthquake Engineering & Structural Dynamics, 34*(10), 1243-1270. doi:10.1002/eqe.478

Krstevska, L. (1996). Experimental dynamic testing of prototype and model of the antonina column in roma.

MAKRIS, N., & ROUSSOS, Y. S. (2000). Rocking response of rigid blocks under near-source ground motions. *Géotechnique, 50*(3), 243-262. doi:10.1680/geot.2000.50.3.243

Mavroeidis, G., & Apostolos, S. (2003). A mathematical representation of near-fault ground motions. *Bulletin of the Seismological Society of America - BULL SEISMOL SOC AMER, 93,* 1099-1131. doi:10.1785/0120020100

Mouzakis, H. P., Psycharis, I. N., Papastamatiou, D. Y., Carydis, P. G., Papantonopoulos, C., & Zambas, C. (2002). Experimental investigation of the earthquake response of a model of a marble classical column. *Earthquake Engineering & Structural Dynamics, 31*(9), 1681-1698. doi:10.1002/eqe.184

Nemer, T., Meghraoui, M., & Khair, K. (2008). The rachaya-serghaya fault system (lebanon): Evidence of coseismic ruptures, and the AD 1759 earthquake sequence. *Journal of Geophysical Research: Solid Earth, 113*(B5), B05312-n/a. doi:10.1029/2007JB005090

Papadopoulos, K., Vintzileou, E., & Psycharis, I. N. (2019). Finite element analysis of the seismic response of ancient columns. *Earthquake Engineering & Structural Dynamics, 48*(13), 1432-1450. doi:10.1002/eqe.3207

Papantonopoulos, C., Psycharis, I. N., Papastamatiou, D. Y., Lemos, J. V., & Mouzakis, H. P. (2002). Numerical prediction of the earthquake response of classical columns using the distinct element method. *Earthquake Engineering & Structural Dynamics, 31*(9), 1699-1717. doi:10.1002/eqe.185

Pitilakis, K., Tsinidis, G., & Karafagka, S. (2017). Analysis of the seismic behavior of classical multi-drum and monolithic columns. *Bulletin of Earthquake Engineering, 15*(12), 5281-5307. doi:10.1007/s10518-017-0160-4

Psycharis, I. N., Papastamatiou, D. Y., & Alexandris, A. P. (2000). Parametric investigation of the stability of classical columns under harmonic and earthquake excitations. *Earthquake Engineering & Structural Dynamics, 29*(8), 1093-1109. doi:10.1002/1096-9845(200008)29:83.0.CO;2-S

Psycharis, I. (2011). Earthquake stability of columns and statues. *Journal of Earthquake Engineering, 15*, 685-710. doi:10.1080/13632469.2010.541549

Sarhosis, V., Asteris, P., Wang, T., Hu, W., & Han, Y. (2016). On the stability of colonnade structural systems under static and dynamic loading conditions. *Bulletin of Earthquake Engineering, 14*(4), 1131-1152. Retrieved from https://eprints.whiterose.ac.uk/146291/

Sarhosis, V., Baraldi, D., Lemos, J. V., & Milani, G. (2019). Dynamic behaviour of ancient freestanding multi-drum and monolithic columns subjected to horizontal and vertical excitations. *Soil Dynamics and Earthquake Engineering, 120*, 39-57. doi:https://doi.org/10.1016/j.soildyn.2019.01.024

Schweppe, G., Reamer, S., & Marco, S. (2021). Reconstructing the slip velocities of the 1202 and 1759 CE earthquakes based on faulted archaeological structures at tell ateret, dead sea fault. *Journal of Seismology, 25* doi:10.1007/s10950-021-10009-0

Sintubin, M. (2011). Archaeoseismology: Past, present and future. *Quaternary International, 242*(1), 4-10. doi:10.1016/j.quaint.2011.03.056

Stefanou, I., Psycharis, I., & Georgopoulos, I. (2011). Dynamic response of reinforced masonry columns in classical monuments. *Construction & Building Materials, 25*(12), 4325-4337. doi:10.1016/j.conbuildmat.2010.12.042

Stefanou, I., Vardoulakis, I., & Mavraganis, A. (2010). Dynamic motion of a conical frustum over a rough horizontal plane. *International Journal of Non-Linear Mechanics, 46*(1), 114-124. doi:10.1016/j.ijnonlinmec.2010.07.008

Tabbara, M. R., & Karam, G. N. (2019). Experimental, numerical, and theoretical investigation of the rocking response of baalbek columns under harmonic excitations. *Journal of Earthquake Engineering : JEE, ,* 1-24. doi:10.1080/13632469.2019.1693448

Tabbara, M., Karam, G., Jello, J., & Beaino, C. (2021). Rocking, wobbling and overturning of the multidrum columns of baalbek under periodic pulses. *Journal of Seismology, 25*(5), 1209-1226. doi:10.1007/s10950-021-10023-2

Toumbakari, E. E., & Psycharis, I. N.Parametric investigation of the seismic response of a column of theAphrodite temple in amathus, cyprus. Paper presented at the *Proc.14th European Conference on Earthquake Engineering, Ohrid,*

Vassiliou, M. F., Burger, S., Egger, M., Bachmann, J. A., Broccardo, M., & Stojadinovic, B. (2017). The three-dimensional behavior of inverted pendulum cylindrical structures during earthquakes. *Earthquake Engineering & Structural Dynamics, 46*(14), 2261-2280. doi:10.1002/eqe.2903

Wald, D. J., Quitoriano, V., Heaton, T. H., & Kanamori, H. (1999). Relationships between peak ground acceleration, peak ground velocity, and modified mercalli intensity in california. *Earthquake Spectra, 15*(3), 557-564. doi:10.1193/1.1586058

Wechsler, N., Rockwell, T. K., Klinger, Y., Štěpančíková, P., Kanari, M., Marco, S., & Agnon, A. (2014). A paleoseismic record of earthquakes for the dead sea transform fault between the first and seventh centuries C.E.: Nonperiodic behavior of a plate boundary fault. *Bulletin of the Seismological Society of America, 104*(3), 1329-1347. doi:10.1785/0120130304